

Application of holographic interferometry for plasma diagnostics

A. N. Zaidel'

A. F. Ioffe Physico-Technical Institute, Academy of Sciences of the USSR, Leningrad
Usp. Fiz. Nauk **149**, 105–138 (May 1986)

The principle of holographic interferometry is described and its importance for plasma diagnostics is indicated, particularly for the determination of electron concentration (Section 2). A review is given of different methods for increasing the sensitivity associated with penetration into the infrared region of the spectrum, and also with the use of multiple-pass, resonance, dispersive nonlinear and two-wavelength holographic interferometry. Section 3 discusses the experimental techniques—recording media and radiation sources—as well as the results of fringe shift measurements, stroboscopic holography and cineholography. Section 4 gives a review of work on investigation of various plasmas—laser-induced sparks, laser jets, neutral current layers, z - and θ -pinches, flash lamps, CO₂ laser-induced plasmas, exploding conductors, plasmotrons, electric arcs and various other kinds of electric discharges in gases.

TABLE OF CONTENTS

1. Introduction.....	447
2. Sensitivity and accuracy.....	448
2.1. Dependence on λ . Infrared holography. 2.2. Multiple-pass holography. 2.3. Higher orders. 2.4. Resonance holography. 2.5. Two-wavelength interferometry. 2.6. Dispersive holography. 2.7. Accuracy.	
3. Experimental techniques.....	453
3.1. Recording materials. 3.2. Optical materials. 3.3. Light sources. 3.4. Cineholography. 3.5. Stroboscopic holography. 3.6. Fringe shift measurements.	
4. Study of plasmas.....	456
4.1. Laser sparks. 4.2. Laser jets. 4.3. Neutral current layers. 4.4. z - and θ -pinches. 4.5. Flash lamp plasmas. 4.6. CO ₂ laser-induced plasmas. 4.7. Plasmotrons. 4.8. Exploding conductors. 4.9. Electric arcs and other types of discharges.	
References.....	464

1. INTRODUCTION

The discovery of holographic interferometry twenty years ago has opened up a number of new possibilities for interferometric studies of a large class of various processes.

By now the method is developed sufficiently well and described in a number of textbooks and monographs.^{1–6} In this article we will discuss briefly the characteristics and details of holographic interferometry that are used in the research on nearly transparent refracting objects such as, for example, plasmas. We consider only the wavelengths from 200 nm to 10 000 nm; other regions of the spectrum have not been used for holographic interferometry of plasma. However, the microwave region can become useful when acceptably good methods for formation and registration of holographic interferograms will be developed for these wavelengths.

The principle of holographic interferometry is based on the recording of two (or more) holograms, corresponding to different states of an object under study, on a photographic emulsion or any other recording material. As a result of interference of waves which correspond to the first and second states of an object, one observes during the reconstruction of such a combined hologram interference fringes that contain information about the light path variations of the hologram-forming beams. In other words, it is possible to calculate a quantity

$$L = \int_0^l [n_1(l) - n_2(l)] dl, \quad (1)$$

from the shape and position of the fringes of a reconstructed holographic interferogram. Here n_1 and n_2 are the refractive indices of the object for different elemental volumes along the probing beam, and l is the light path within the material under investigation (the indices 1 and 2 refer to the state of an object during the first and second exposures).

The conditions of the experiment can usually be chosen in such a way that $n_2 = 1$; then, by reconstructing the holographic interferogram at different angles, it is possible in principle to work with local values of k in various areas of the object under study instead of the integrated quantity L . Unfortunately, this approach leads to a significant decrease in the accuracy of measurements so that local values of n can be determined with much less accuracy than the integrated quantity L .

The principle described above corresponds to so called double-exposure holographic interferometry. In general, the term “holographic interferometry” is used to describe any method involving the observation of an interferogram in which at least one (or both) of the interfering waves is reconstructed with the help of a hologram. The second wave can be, for example, a wave directly scattered by the object under study (the real-time method). It is double-exposure interfer-

ometry that is used most often in the study of plasma objects. Holographic interferometry, like conventional interferometry, makes it possible to find the refractive index volume distribution for the object under study. The holographic method, however, has some advantages which have stimulated its development over the last several years. Among these advantages we note in particular the following:

1. By reconstructing a double-exposure holographic interferogram, we can observe interference of two waves passing through the object at different times.

2. The reconstruction of a holographic interferogram at different angles allows one to use the local values of n instead of the integrated values L . Application of conventional interferometry to objects without axial symmetry would require the use of several interferometers and of many interferograms obtained by illuminating the object at different angles.

3. Since there is no need in this case to use high quality optics, this not only makes the experimental arrangement cheaper but also allows us to study large volumes of plasma in chambers with transparent windows and walls made from not very high quality optical materials. This is explained by the fact that in holographic interferometry any distortions of the wavefront caused by optics are compensated. An interference pattern registers only those phase inhomogeneities that appear during the time intervals between two exposures.

One should keep in mind that the optical inhomogeneities of a chamber wall on the hologram side can influence to some extent the shape of the fringes observed during reconstruction, but in the usual and not in the "interference" sense, since these fringes are reconstructed in the same form as they are seen through this wall. If the wall is so nonuniform that it significantly distorts the shape of the fringes or, even more, if the fringes are not visible through the wall because it diffusely scatters the light, then it is necessary to use special methods to reconstruct the holograms. In one such method, for example, the image of a wall is aligned with the wall itself (see details in Ref. 6 for example, pp. 414-422). The distortions caused by the wall or window deformations as a result of thermal heating by a pulsed plasma can certainly have an influence on the position of the interferometric fringes, and one should always consider this possibility.

4. Holographic interferometry makes it possible to observe surprising two-wavefront interference patterns, whose shape corresponds to distortions introduced by the object, when the holograms are created by illuminating radiation at different wavelengths. In other words, it seems as if one can observe a stationary interference pattern arising as a result of the interaction of two waves with significantly different wavelengths (for example, by a factor of two or three).

Finally, holographic interferometry opens up entirely new opportunities for increasing the sensitivity of interferometric measurements.

Consideration of these advantages has led to a number of plasma diagnostics experiments using the holographic interference method for various kinds of plasmas under study at the A. F. Ioffe Physico-Technical Institute in 1965-1966^{7,8} followed by similar research in the United States.^{9,10}

Later these methods were further developed in a number of laboratories, and several review papers have been written.^{11,12} Holographic interferometry has turned out to be a method which makes it possible to obtain a number of interesting results that could not be achieved practically by other techniques.

Analysis of holographic interferograms gives the distribution (spatial, as well as temporal) of the plasma refractive index, which is related to the concentration of electrons, atoms and ions that make up the plasma. The final goal of interferometric measurements is the determination of the concentrations of these particles.

2. SENSITIVITY AND ACCURACY

The sensitivity of the holographic interferometry method is determined by the lowest concentration of particles (electrons and atoms) that can be detected with this method. In order to estimate this quantity we start with the fact that, without using the special methods (described below) to increase the sensitivity of the hologram, changes in the light path difference that are less than 0.1λ cannot be detected. On the other hand, it is difficult to register optical path changes larger than 100λ (for one object).

2.1. Dependence on λ . Infrared holography

In general, the refractive index of a plasma far from any atomic absorption lines can be calculated from the Cauchy formula:

$$n - 1 = \sum_{i=1}^k \left(A_i + \frac{B_i}{\lambda^2} \right) N_{a_i} - 4.5 \cdot 10^{-14} \lambda^2 N_e, \quad (2)$$

where N_e is the electron concentration and N_{a_i} is the atomic concentration. In most cases the contribution of ions to the total refractive index of the plasma can be neglected.

Using for the A and B constants in the Cauchy formula their values for air, we find that the absolute value of the refractive index of air is comparable to the refractive index of the electron gas when the ratio of the particle concentrations is

$$\frac{N_e}{N_a} \approx 0.1. \quad (3)$$

On the other hand, a variation of the optical path of 0.1λ (for $\lambda = 500 \text{ nm}$) corresponds to a surface electron concentration of $5 \times 10^{16} \text{ cm}^{-2}$. This determines the minimal electron concentration that can be measured by holographic methods (for $l = 1 \text{ cm}$ $N_e = 5 \cdot 10^{16} \text{ cm}^{-3}$). It follows from equation (3) that the minimal atomic concentration is approximately a factor of 10 larger. An increase in interferometric measurement sensitivity leads to a corresponding decrease in the lower limit of detectable concentrations.

A quantity that is determined during interferometric measurements of the refractive index is the fringe shift K caused by introducing an optical path difference. For plasma this shift is related to the concentration of plasma particles by the expression

$$K = \frac{n l}{\lambda} = \left[\sum_{i=1}^k \left(A_i + \frac{B_i}{\lambda^2} \right) - 4.5 \cdot 10^{14} N_e + 1 \right] \frac{l}{\lambda}. \quad (4)$$

Let us assume that the smallest detectable fringe shift ΔK is 0.1 of the distance between fringes. (This is usually a realistic assumption for holographic interferometry.)

Assuming that $A \gg B$, we obtain from Eqs. (2) and (4) for the minimal detectable shift of ΔK of fringes in a pure electron gas the relationship $\Delta K \sim \lambda$, and, correspondingly, $\Delta K \sim 1/\lambda$ for a gas consisting only of atoms.

Obviously, in moving into the infrared region of the spectrum, the sensitivity of the interferometric method for determining N_e increases, while the corresponding lower limit on the atomic concentration N_a decreases.

When a CO_2 -laser, instead of a ruby laser, is used for plasma probing, the expression (3) changes to

$$\frac{N_a}{N_e} = 2 \cdot 10^3. \quad (3')$$

Thus, the influence of an atomic (molecular) gas on the plasma refraction coefficient can often be neglected.

Development of this method has been delayed until recently by difficulties in recording holograms and designing optical systems in the infrared region of the spectrum, and only in the last several years has it become possible to obtain encouraging results. The use of a CO_2 -laser made it possible to achieve approximately a 15-fold increase in the sensitivity measurement of $1/N_e$ compared with the ruby laser results, and to determine $1/N_e$ down to $2 \cdot 10^{15} \text{ cm}^{-2}$ (Refs. 15, 16); in addition, by using nonlinear recording of holograms (including fifth to eighth orders), the detectable value of $1/N_{e, \text{min}}$ drops down to $\approx 2 \cdot 10^{14} \text{ cm}^{-2}$, which as the authors note, makes it realistic to use holographic interferometry for plasma diagnostics in installations of the tokamak type. Experimental instrumentation for this type of research has already been built, and preliminary experiments have demonstrated that it has a rather high sensitivity.^{17a}

Recently the development of an interferometric apparatus was reported which uses a CO_2 laser to determine $1/N_{e, \text{min}}$ down to 10^{13} cm^{-2} . The smallest shift that can be detected with this apparatus is 1/50 of a fringe width.^{17b}

Some details of applications of infrared holographic diagnostics are described in Refs. 18, 19.

When the visible region of the spectrum ($\lambda = 500 \text{ nm}$) is used, the concentration range over which holographic interferometry methods are applicable is limited from below by difficulties in determining small fringe shifts, and from above by the reflection, absorption and scattering of the probing light. These phenomena are beginning to become noticeable for $N_e > 10^{20} \text{ cm}^{-3}$. Thus, for a plasma with linear dimensions of the order of 1 cm, the concentration range N_e that can be measured with the help of visible light is approximately $10^{16} - 10^{20} \text{ cm}^{-3}$.

Originally holographic methods were developed for studying plasmas in thermonuclear fusion installations. For this reason, it was important to extend the range of measurements toward smaller concentrations down to $N_e \sim 10^{13} \text{ cm}^{-3}$ (tokamaks) and toward higher concentrations up to $10^{22} - 10^{24} \text{ cm}^{-3}$ (laser-induced thermonuclear reactions).²⁰ There is an equally great interest, however, in research on relatively cold and dense plasmas for which the refractive index is determined mainly by the refractive indices of the

atomic and molecular gases. A large amount of research, therefore, is devoted to the study of plasmas in electric arcs, plasmotrons, gas discharges, etc. Much effort has been directed towards finding methods to study plasmas with low values of N_e .

To minimize the electron concentration that can be detected by holographic methods one should search for methods which increase the optical path difference caused by changes in the refractive index. Holographic methods provide researchers with several different ways, in addition to using the infrared areas of the spectrum, to approach this goal.

2.2. Multiple-pass holography

First of all, we will mention the use of the multiple passage of a probing beam through the plasma, a method which is used also in regular holography. Figure 1a shows the corresponding optical arrangement.

To obtain holograms with a K -fold beam passage through a plasma it is necessary to separate spatially the beams corresponding to different numbers of passes through the plasmas. This can be achieved by slightly tilting the semi-transparent mirrors 3 and 4 relative to each other. The diaphragm 1 placed in the focal plane of the lens 2 selects a beam with a given number of passages. Other beams continue to probe the plasma at various points, thus decreasing the spatial resolution of the method. In holographic interferometry the selection of the required beam can be done without tilting the mirrors 3 and 4 (Fig. 1b).^{21,22} This is due to the fact that among several beams passing through a plasma only those beams will form a holographic interferogram for which an optical path $2nKd + a_1 + a_2$ differs from $b_1 + b_2$ by not more than a coherence length L of the probing laser radiation. The width $\Delta\nu$ of the generating line can be chosen in such a way that the coherence length is less than $2nd$; then

$$2nd \geq L \approx \frac{c}{\Delta\nu}; \quad (5)$$

here c is the speed of light and, $\Delta\nu$ is the width of the generation line.

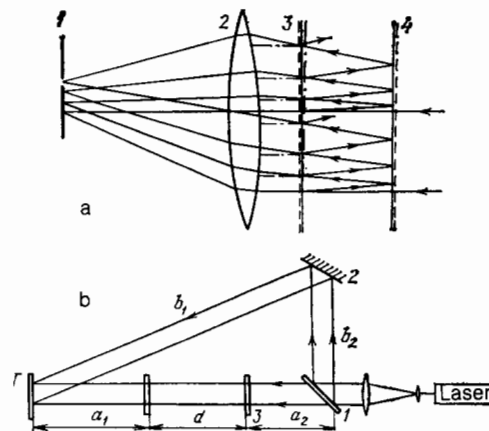


FIG. 1. Sensitivity increase by multiple-pass method. a) Tilted mirrors; b) parallel mirrors.

If $d = 15$ cm and $n = 1$, then $\Delta\nu$ must not be larger than 1000 MHz, i.e., for the visible part of the spectrum $\Delta\lambda$ is about 0.01 \AA . The beams that do not satisfy the condition (5) will not interfere; however, they give rise to additional exposures of the hologram, which worsens the quality of the interferograms; this deterioration in quality increases with an increase in the number of passages that is selected.

In order to choose the specified number of passages, one must, by varying the relative positions of the mirrors 1 and 2, change b_1 and b_2 in such a way as to satisfy the condition

$$b_1 + b_2 - (a_1 + a_2 + 2Kd) < 2d$$

(here, of course, one can put $n = 1$).

One must take into account that during multiple reflection of a beam from the mirrors 3 and 4 the wavefront distortions introduced by the mirror defects are accumulating. For this reason, the mirrors 3 and 4 in the multiple-pass scheme must have a surface finish not worse than $(0.1-0.05)$, while in order to form regular holographic interferograms it is sufficient to have optics made with a precision not better than 0.5λ . The required number of passes is selected by using a compromise between a desirable sensitivity increase and the degree of deterioration in interferogram quality taking place with an increase of K . If the duration of a probing pulse is τ , and the time taken for a single pulse to go through a plasma is τ' , then after many passes of a beam it may occur that $K\tau' \gg \tau$. The temporal resolution of the multiple-pass method will then be by a factor $1 + (K\tau'/\tau)$ smaller than the resolution of a single-pass method. On the other hand, $1 + (K\tau'/\tau)$ can significantly exceed 1 only when picosecond probing pulses are used.

2.3. Higher orders

Another method of increasing sensitivity is based on nonlinear effects observed in holograms for most photosensitive materials. It is known that during reconstruction of such holograms one can observe, in addition to the zeroth and first order images also images corresponding to the higher orders of diffraction. If we observe an image of K th order, then all distortions of the beams forming the image will be K times larger than for the first order waves (Fig. 2). In order to reconstruct a hologram, we illuminate it with two mutually perpendicular beams tilted relative to each other by such an angle β that the K th order wavefront reconstructed by the first beam coincides with the R th order wavefront reconstructed by the second beam (Fig. 3a). The best approach is to choose a symmetrical position of the reconstructed beams relative to the normal to the hologram. This leads to a $2K$ -fold increase in fringe shifts compared to the usual reconstruction method. Obviously, one can select the directions of the reconstructing beams in such a way so that the wavefronts of the $+N$ th order and $-M$ th order coincide, and this will increase the fringe shift by a factor of $N + M$. The quality of the interferograms produced in this manner, however, is best for the symmetric scheme (Fig. 3b).¹⁴ In this case a single-exposure holographic interferogram obtained as a result of reconstructed wavefront interactions has fringe displacements that are $2K$ times larger than the displacements observed during formation and re-

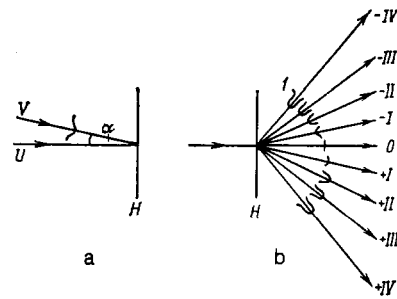


FIG. 2. Formation (a) and reconstruction (b) of holograms in different orders. Marks of the type indicated by the number 1 show wavefront distortions (on an arbitrary scale).

construction of the usual double-exposure interferograms in the first order. If in this case the measurement accuracy of the fringe shifts is the same for both methods of hologram reconstruction, the sensitivity of electron concentration determination is increased by a factor $2K$ for nonlinearly registered holograms. The use of nonlinear effects to increase the sensitivity of holographic interferometry was suggested in Refs. 24, 25. A disadvantage of this method is that the images reconstructed in high orders have distortions the magnitude of which depends on the specific conditions of the experiments. In particular, as is the case for the multiple-pass method, the influence of the hologram-forming optics defects increases in proportion to the method's sensitivity. Therefore, it is recommended to use in this method mirrors and lenses of interferometric quality ($\approx 0.1-0.01 \lambda$).

The optical distortions are minimal if one is using holograms of the focused images for which the planes of an object image and fringe localization coincide (see, for example, Ref. 1). In Ref. 26 the reconstructed 7th order images were used, and in Ref. 27—even images of the 8th order. By combining a multiple passage of a probing beam through the object and reconstruction in higher order, it became possible

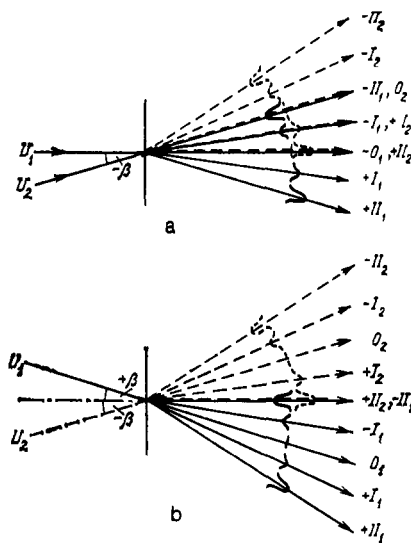


FIG. 3. Reconstruction of a single-exposure holographic interferogram with an asymmetric (a) and a symmetric (b) beam.¹⁴

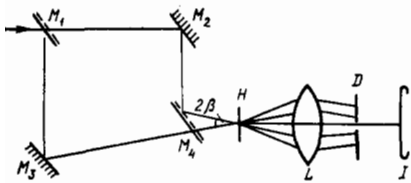


FIG. 4. Reconstruction of a single-exposure holographic interferogram in the ± 2 orders. M_1 - M_4 —semitransparent mirrors; H —hologram; L —lens; D —diaphragm; I —photoemulsion. The planes H and I are conjugated. Lines indicate optical beam axes.

to increase the sensitivity of holographic measurements by a factor of 36.²⁸

Figure 4 shows a possible optical scheme for the reconstruction of a nonlinear interferogram.

2.4. Resonance holography

A substantial sensitivity increase for determination of heavy particles (atoms or ions) concentration in plasma can be achieved by using large changes of refractive index in the vicinity of the absorption lines of the studied atoms, where the refractive index is described by the Sellmeir formula.

$$n - 1 = R \frac{N_a^* \lambda_0^3}{\lambda - \lambda_0}; \quad (6)$$

where R is a constant depending on the atomic constants, λ_0 is the absorption line wavelength, N_a^* —the population of the initial level of the absorption line. Near the absorption line the refractive index can exceed the refractive index in the area of normal dispersion by several orders of magnitude. Correspondingly, the sensitivity of atomic or ionic concentration measurements also increases.

In the first work using the resonance holography method, the choice of laser lines close to atomic absorption lines was very limited,^{29,30} and one had to use special methods to shift laser lines. It was done, for example, by changing the temperature of the ruby crystal³¹ or using Raman spectra.²⁹ The situation has changed significantly since the development of dye lasers which allow a continuous change of the laser wavelengths. Dye lasers made it possible to study a large class of atoms and to use successfully resonance methods both for conventional and holographic interferometry.^{32,33}

The calculations of a sensitivity increase that can be achieved with resonance holography were carried out in Ref. 31 (see also the more detailed calculations in Ref. 33). From these calculations it follows that the minimum of detectable concentration is achieved when the distance between centers of the probing and absorption lines is equal to the half-width of the absorption line. Figure 5 shows the sensitivity variation curves for an infinitely narrow probing line as a function of the distance from a probing line of finite width.³³ As can be seen from the graph, the lowest atomic concentration that can be detected for an absorption line with the oscillator strength $f = 1$ in the case of a transilluminated layer with the thickness of 1 cm is $\approx 2 \cdot 10^{12} \text{ cm}^{-3}$.

2.5. Two-wavelength Interferometry

From equation (2) it follows that in order to determine the electron density N_e from the measured values of n it is

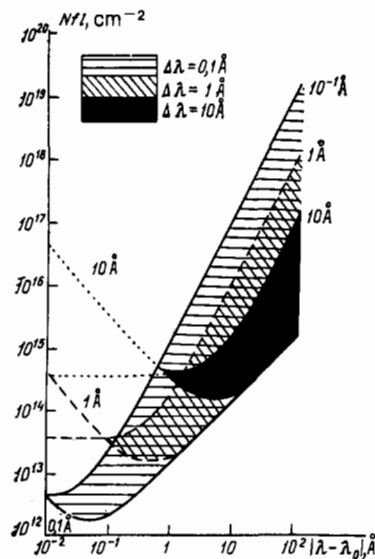


FIG. 5. Applicability regions of resonance holographic interferometry.

necessary to eliminate the heavy particle influence on the plasma refractive index. This can be achieved by measuring values of the refractive index for several different wavelengths and then finding the atomic N_a and electron N_e concentrations by solving equation (2).

By substituting the values of A and B into equation (2), it is easy to see that when λ changes by a factor of two the part of the plasma total refractive index due to heavy particles changes by 5–10%, and the part due to the electron gas changes by a factor of 4. From this fact it follows that the plasma dispersion ($dn/d\lambda$) depends practically only on N_e . In other words, the differences of the interferogram fringe shifts for two different wavelengths (far from the absorption line) enables one to obtain directly the values of IN_e .

The development of the two-wavelength conventional³⁴ and holographic³⁵ interferometry is based on these ideas. In order to obtain holograms for two different wavelengths, it was customary to use, as was done in these and the following works, the frequency doubling of a probing radiation using a nonlinear crystal. The object was illuminated by a mixed beam consisting of the main frequency radiation and its harmonic, and this led to the formation of two spatially separated holograms. During reconstruction of these two holograms one obtains two spatially separated holograms simultaneous analysis of which allows one to determine both the electron and atomic concentration.

If heavy particles contribute significantly to the refractive index, then the fringe shifts caused by an electron gas are calculated as small differences of large shifts introduced by plasma for the wavelengths λ_1 and λ_2 . One must also take into account that during the reconstruction of the two holograms, it is possible, as a result of some difference in the image size and variation of aberrations, to have different errors in determining the position of points used for the shift measurements for the main and doubled frequencies. All these reasons lead to a situation that (in this case) the accuracy of concentration determination from two interferograms is significantly smaller than for the case when the

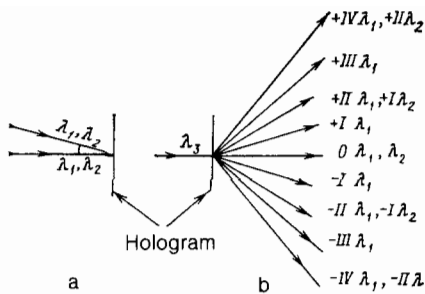


FIG. 6. a—Formation of a dispersive hologram; b—reconstruction of a dispersive hologram.

contribution of heavy particles to a refractive index can be completely neglected.

A method automatically eliminating the shifts caused by heavy particles was considered in Ref. 36, where it was suggested to use for this purpose the nonlinear properties of holograms.

2.6. Dispersive holography

Let us consider a plasma illuminated with a beam containing coherent radiation with the wavelengths λ_1 and $\lambda_2 = 0.5\lambda_1$, and assume that a reference beam is formed by the radiation with the same composition (Fig. 6a). Two overlapping holograms are formed first in the plane P and then are reconstructed by the radiation with a wavelength which, generally speaking, can be different from λ_1 and λ_2 . The frequency of the interference fringes on the "blue" hologram is twice as large as the frequency on the "red" hologram. For this reason a wavefront for a wavelength λ_2 reconstructed in the first order coincides with the wavefront for λ_1 in the second order. In exactly the same way, the wavefronts of the second and fourth diffraction orders, etc., coincide (Fig. 6b). The wavefronts reconstructed in the first and second orders interfere and form a single-exposure holographic interferogram on which all fringe shifts are determined by a

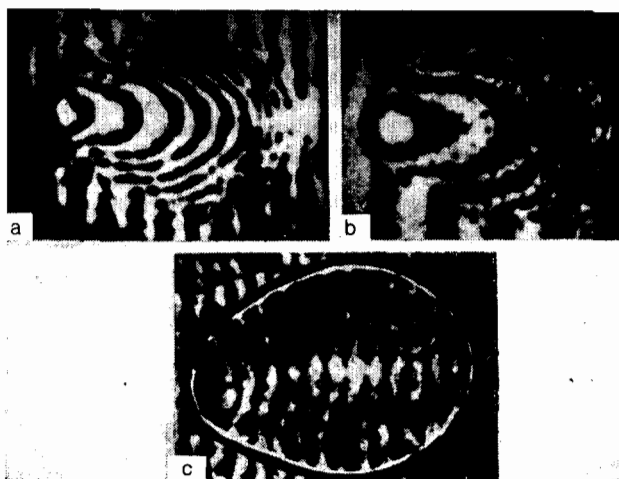


FIG. 7. Two-wavelength holographic interferograms [$\lambda(\mu) \approx 0.35$ (a) and 0.69 (b)] and dispersive interferogram of a laser spark (c).⁴⁰

difference between refraction indices n_1 and n_2 for the wavelengths λ_1 and λ_2 (Fig. 7).

A significant advantage of the described method is that the two compared waves are obtained not in two but in a single exposure. This helps to avoid experimental errors caused by a change of the experimental apparatus position during the time interval between two exposures. An experimental apparatus in this case becomes therefore much less sensitive to vibrations and deformations than an experimental apparatus for double-exposure holographic interferometry. This is also true in equal measure for the method of reconstructing waves in higher orders of a single-exposure nonlinear hologram. Naturally, all the disadvantages noted in the discussion of the latter method of increasing the sensitivity are also inherent in dispersive interferometry.

In order to obtain good dispersive interferograms one must also take special care in selecting photomaterials with an appropriate spectral sensitivity curve. It is important to try to achieve that the darkened areas in the first order for λ_1 would be close to the darkened areas in the second order for λ_2 (and the same for the 2nd and 4th orders, respectively, etc.). Of course, color filters can be used to make the distribution of the darkened areas more uniform. Another source of errors can also be a size difference of the reconstructed images corresponding to the wavelengths λ_1 and λ_2 . For this reason, it is better, probably, to use for the reconstruction radiation with a wavelength λ_3 satisfying the condition $\lambda_2 < \lambda_3 < \lambda_1$. The details of the analysis of the applicability conditions and properties of dispersive holography are considered in Ref. 37.

A device called the dispersive interferometer has been specially designed to produce dispersive interferograms.^{38,39} Various schemes of dispersive interferometers are considered in Ref. 40. The working principle of interferometers of this type is shown in Fig. 8.

An object O being investigated is placed between two nonlinear crystals K_1 and K_2 in which a frequency shift takes place. The filter Φ that selects the sum frequency $\omega_3 = \omega_1 + \omega_2$ is placed after the element K_2 . If the element K_1 is illuminated with a beam containing the frequencies ω_1 and ω_2 , the object O will be irradiated by the waves U_1 , U_2 and U_3 with the frequencies ω_1 , ω_2 and ω_3 , respectively. All these waves experience the wavefront distortions which are proportional to the optical path difference introduced by the object into each wave. Further, the waves U_1 , U_2 and U_3 pass through an identical crystal K_2 where the waves U_1 and U_2 are mixed and thus generate the wave U'_3 . All the beams pass through a light filter Φ which transmits only the radiation with the frequency ω_3 . The two wavefronts: U_3 , which passes through the crystal K_2 without a frequency change, and U'_3 , which is obtained as the result of mixing of the waves U_1 and U_2 in the crystal K_2 , interfere. Finally, an interferogram is

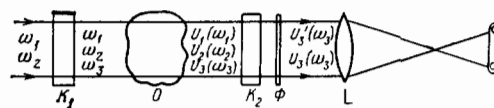


FIG. 8. Scheme of a dispersive interferometer.

observed in the focal plane of the objective L placed after the filter. The shifts of the interferogram fringes are determined only by the difference of the object refractive indices at the frequencies ω_1 and ω_2 . A particular case of the application of this approach is an interferometer (described in Ref. 38) based on the principle of frequency doubling ($\omega_2 = 2\omega_1$). Such a device has already been constructed and used to produce interferograms (see Fig. 7). If one of the mixed frequencies ω_1 , for example, is chosen to be small, then the sensitivity of interferometric measurements of N_e can be significantly increased by using the infrared region for probing radiation, and registering the interferograms in any convenient region of the spectrum. So far, probably, only purely technical difficulties have been preventing the realization of this idea.¹⁾

2.7. Accuracy

The accuracy of measuring the concentration using the holographic interferometry method is determined ultimately by the accuracy of measuring the magnitude of the interference fringe shift. Usually, it is assumed that this accuracy is one tenth of the distance between fringes.

A statistical analysis of various kinds of experimental errors in holographic interferometry was made in Ref. 41. In addition to the sources of error common to all applications of holographic interferometry, in the investigation of plasmas there is a number of specific causes reducing the quality of interferograms and, correspondingly, the measurement accuracy:

1. The exposure of holograms to incoherent plasma radiation reduces their diffraction efficiency;
2. All methods in which several holograms are overlapping also lead to a reduced diffraction efficiency;
3. If an illuminating pulse is not sufficiently short, interference fringes become "smeared" because of the change of $N_e l$ during irradiation; this can lead to a complete "blurring" of the hologram, as was observed, for example, during the study of super-high pressure lamps.^{8,12}

In Ref. 42 the measurement accuracy of fringe shifts in nonlinear holograms has been studied. The dispersion of experimental errors σ was 0.2 of the distance between fringes, which is slightly larger than the assumed value of 0.1. This deviation can be easily explained by an interferogram quality decrease observed in the case of reconstruction of higher order waves. On the other hand, when the quality of fringes is good and when photovoltaic registration is used, it is possible to measure a shift of 0.01 of the distance between fringes and even less. If one assumes that the largest shift over the extent of the studied object is about 10 fringes, then the minimal relative experimental error is approximately 0.1–1%. In practice, it is usually larger for a combination of the reasons given above and is around 10–20%, and in some cases only an order of magnitude $N_e l$ can be estimated.

3. EXPERIMENTAL TECHNIQUES

3.1. Recording materials

It is well known that, in addition to amplitude holograms which register spatial variations of incident radiation,

there are also phase holograms that work by changing the phases of light waves passing through the various areas of a hologram. Sometimes phase-amplitude holograms, which simultaneously modulate the amplitude and phase of a reconstructed beam are used.

The most widely used technique, i.e., recording interferograms on a photographic plate, yields only amplitude modulation, although there is some phase-modulation contribution due to changes in the gelatine layer surface texture. In selecting a recording material, it is necessary first of all to take into account the material's sensitivity to the radiation of a given spectral composition, and the material's resolution capabilities (the number of lines that can be recorded separately on one millimeter of the material).

Usually these two properties compete with each other, and materials with a high sensitivity have a lower resolution, and vice versa. For some recording media, the images formed in them disappear very fast, which obviously creates additional difficulties. The most widely used recording medium for the visible and near ultraviolet regions is photoemulsion.

The frequency of hologram interference fringes is determined by the formula

$$\nu = \frac{2 \sin(\alpha/2)}{\lambda}, \quad (7)$$

where α is the angle between interfering beams.

Obviously, in order to have images without distortions due to the limited resolving capabilities of recording materials, the resolution of a hologram must generally be larger than ν . Since the angle between the object and reference beams used in the holographic interferometry of plasmas usually does not exceed several degrees, the frequency of hologram fringes will not exceed 100 lines/mm, and sometimes is significantly less for the infrared region. Special holographic photographic emulsions have a very high resolution (up to 5000 lines/mm) and a low sensitivity not exceeding several hundred $\mu\text{J}/\text{cm}^{-2}$ [0.1–10 GOST (State All-Union Standard) units].

For holographic interferometry of plasmas, materials with a resolution of 100 lines/mm and high sensitivity (for example, the film PANCHROM-18) have been used successfully.

For recording of holograms in the infrared region, materials the optical properties of which change under the influence of irradiation are usually used. Most often this change is caused by the melting or evaporation of the surface. Sometimes the phase transitions caused by heating are also used. The sensitivity and resolution of such layers is usually less than those for photographic emulsions, which, unfortunately, are not suitable for $\lambda > 1200$ nm. Table I lists some of the materials that have been used for the recording of holograms obtained with the help of the CO_2 -laser ($\lambda = 10.6 \mu$). The table also contains the main parameters of the layers made from these materials.

3.2. Optical materials

Holographic instrumentation designed for research in the visible region can use regular optical materials. For the

TABLE I. Recording materials for infrared holograms.

Material	Recording mechanism	Sensitivity	Resolution (lines/mm)	References
Bismuth film	Evaporation	0.3	100	43
Gelatine	Melting	0.2	20	44
	Burning	2	300	45
Paraffin	Melting	0.4	40	46
	Melting	0.1	20	47
Liquid crystals	Phase transition	$5 \cdot 10^{-9}$	500	48
Ftiros*	Same	0.1-0.01	50	49
Silver halide emulsion**	Thermal			

*Ftiros—a relatively new recording material developed in the Physico-Technical Institute of the Academy of Sciences of the USSR, the working principle of which is based on the phase transition caused by heating.

**Recording mechanism is based on the sensitivity increase of a photoemulsion to the visible radiation when it is heated by infrared radiation.

infrared region, special mirrors and lenses should be used for particular areas of the infrared spectrum. For the 10.6 region the best mirror coating material is copper that has a reflection coefficient of 98.4%; Pt, Rh, Ag, Au also have high reflection coefficients (94–96% reflectance). Occasionally, aluminum mirrors are used even though the aluminum reflection coefficient is 90%.⁵⁰ For $r = 0.9$, the overall reflection losses are increasing rapidly for a large number of surfaces. In addition, the large amount of energy absorbed in a reflecting layer can lead to its damage.

Lenses and optical windows can be made from crystals of BaF_2 , PbF_2 , KPS-6 (40% TlBr , 60% TlCl), KRS-13 (60% AgBr , 35% AgCl) and others. Germanium, having the refractive index 4 for the wavelength of 10μ , is especially convenient for making beam splitters that divide a beam into two beams of approximately equal intensity. In order to avoid secondary reflections, such beam splitters are made in the shape of wedges.

It must be remembered that the optics used for the CO_2 lasers can be manufactured with 10–15 times less accuracy of polishing than the optics for the visible region of the spectrum (this is due to a significant difference of the wavelengths involved).

3.3. Light sources

The formation and reconstruction of holographic interferograms is usually done with lasers, although the use of lasers, in general, is unnecessary for reconstruction. Depending on the object being investigated, the requirements on the characteristics of the lasers employed vary significantly. Only in a few rare cases is a plasma sufficiently stationary so that one can use CW lasers for its study; as a rule, pulsed lasers are used, with the duration of the probing pulse having to be adjusted to the rate of change of the plasma parameters. In most cases the best lasers for the visible region of the spectrum are the ruby or neodymium lasers working in the free generation mode in the case of slowly changing plasma parameters and in the Q -switching mode for a highly unstable plasma, with the pulse duration of approximately $100\mu\text{sec}$ or 10–30 nsec, respectively. Over the last several years picosecond lasers operating both on the

main frequency or its harmonics are increasingly often used for this purpose.

It should be remembered that, as a rule, the spatial and temporal coherence properties of the ruby lasers operating in the free generation mode are not adequate for producing holographic interferograms. In order to improve the laser characteristics mode selection is used. The same approach must be used also for dye lasers that at the normal conditions generate a wide spectral band (see details in Ref. 51).

Of the domestically manufactured lasers, the OGM-20 laser is probably the most convenient; its parameters are: $\lambda = 694.3\text{ nm}$, power—20 mW, pulse duration—20 nsec, the angle of divergence— $2'$.⁵² In cases when the laser power is insufficient, optical amplifiers have to be used with an OGM-20 laser serving as the master oscillator.

The most convenient lasers for resonance holography are liquid dye lasers. They make it possible to obtain radiation of any wavelength in the visible and near ultraviolet regions of the spectrum. The power and coherence of these lasers are sufficient for solution of many problems. We have successfully used a "home-made" laser³² that is a modification of the commercial laser "Raduga." For the reconstruction of holograms He-Ne lasers are usually used. Practically, any model of the He-Ne laser can be used (i.e., models LG-36, LG-38), since all have sufficient power and coherence. These lasers are usually included in all holographic systems among the equipment intended for alignment of the parts and adjustment of the entire apparatus.

Application of He-Ne lasers ($\lambda = 632.8\text{ nm}$) for the reconstruction of holograms obtained with another wavelength introduces, of course, some distortions on a scale that is sometimes undesirable.

It must be noted that gas lasers have an excessive coherence for reconstruction of holograms, and in practice it is possible to use broad band light sources, i.e., high pressure mercury lamps with proper optical filters. Still, if a laser is available in a laboratory involved in holographic interferometry, it is an especially convenient source for reconstruction of holograms.

Most often infrared holograms are formed by CO_2 -lasers with a transverse electric discharge pumping

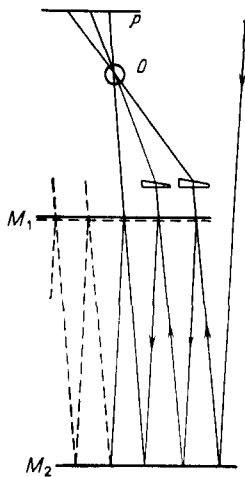


FIG. 9. Optical delay line for the formation of cineholograms. M_1 , M_2 —mirrors; O —object; P —hologram.

(see, i.e., Ref. 53). The main wavelength of the generated radiation is 10.6μ . Sometimes also a pulsed HF-laser with the wavelength of 3μ was used.⁵⁴

3.4. Cineholography

In order to study plasma dynamics it is necessary to obtain a number of holograms or interferograms shifted relative to each other in time. For this purpose, a number of techniques based on the time delay of the probing pulses^{11,55} or on the continuous optical sweeping of a hologram⁵⁶ have been developed. Depending on the typical plasma rise time, various delay methods are used. Several synchronized lasers⁵⁷ or lasers generating a series of giant pulses are used for delays of the order of several microseconds.⁵⁸ Delays of 10^{-6} – 10^{-9} sec can be obtained easily by using the optical delay lines suggested in Refs. 59, 60 that make use of the reflection of light from two mirrors, one of them semitransparent, placed at a specified distance from each other (Fig. 9). The quality of these mirrors must be sufficiently high, since multiple reflections increase the influence of mirror defects on wavefront distortions.

This approach was used for the first time to form cineholograms in Refs. 7, 55. Optical delay lines with another, more convenient arrangement of optical elements, were independently suggested and described in Refs. 61, 62 (see details in Ref. 63). For delays of 10–100 nsec the distance between the mirrors must be several meters. A compact delay line with spherical mirrors has been suggested in Ref. 64. The very large number of reflections in such lines, however, leads not only to strong attenuation of the beam, but also to significant distortion of the wavefront. Other techniques which produce pulses shifted in time have also been developed, including the use of various areas of a laser rod which turn on sequentially; this allows one to study processes lasting several microseconds.⁶⁵ By using delay lines with mirrors, it was possible to form cineholograms containing 3–7 frames.

A disadvantage to this type of scheme is an almost unavoidable decrease of beam intensities with an increase in the

number of reflections, so that the last frame receives significantly less light than the first frame. This situation can be avoided by using mirrors with transmission and reflection coefficients that vary along the surface. Optical pulses of uniform intensity can be obtained by using a laser that produces a series of nanosecond pulses at regular intervals.⁶⁶

3.5. Stroboscopic holography

Stroboscopic holographic interferometry has been suggested for the study of periodic processes and was applied, for example, to the study of gas discharge plasmas.⁶⁷ This method produces a double-exposure interferogram, with each exposure corresponding to a specific stage of the process (for example, to the maximum in the discharge current and to its zero value). As an example, we describe an experimental apparatus for studying a gas discharge plasma, which uses a CW He–Ne laser. In order to protect the apparatus from vibrations, it was placed in a basement on a concrete slab separated from a table by two automobile inner tubes pumped up to a low pressure. All parts of the apparatus were fixed to the rail of an optical bench rigidly attached to the slab. Under these conditions, we did not experience interference due to vibrations even for long exposures.

Several different types of gas discharge lamps were chosen as stationary objects. The first experiments were carried out using a PRK-4 lamp. A diagram of the experimental arrangement is shown in Fig. 10. The light from a He–Ne laser was modulated by a disk with holes. The rotating disk was spun in phase with the current pulses providing power to the lamp. The film was exposed during current interruptions and also when the current was reaching its maximum. A study of holograms has shown that changes in the index of refraction caused by the current led to a variation of the optical path difference at the center of the lamp which was less than λ . This corresponds to a variation in the atomic concentration of mercury along the axis of the discharge which was less than 10%.

The lamp was placed within a case filled with helium in order to exclude the influence of air flows on the index of refraction.

3.6. Fringe shift measurements

An interference fringe on a double-exposure holographic interferogram is a line of constant optical path difference, introduced by the phase object during the interval between two exposures. An example of such an interferogram is

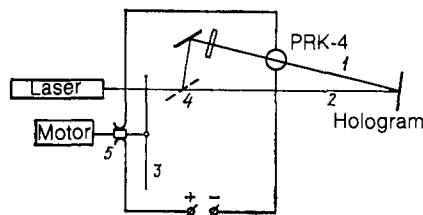


FIG. 10. Stroboscopic holography study of a PRK-4 lamp. 1—object beam; 2—reference beam; 3—interrupting disk; 4—beam splitter; 5—current interrupter.

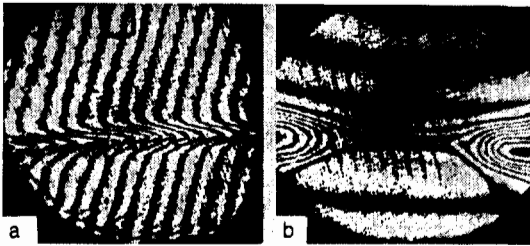


FIG. 11. Interferograms: with a wedge (a) and without a wedge (b).⁹⁹

shown in Fig. 11b. To find the index of refraction (or, more accurately, its change during the interval between two exposures) is very difficult, since there are no convenient reference points for a measurement of the magnitude of the shift. The situation changes if, together with a change in the phase object, one changes slightly the direction of one of the beams (reference or object beam) during the interval between exposures. Rotation of the reference beam through a small angle α leads to the appearance on an interferogram (in the absence of changes in the phase object) of a system of rectilinear interference fringes with a distance between them of $h = (\lambda/2) \sin(\alpha/2)$. If in addition to the tilting of the beam the object introduces a change in the optical path difference, then this will lead to a corresponding distortion of the interference fringes (Fig. 11a). Measurements of the optical path differences introduced by the object are carried out at a number of points on an undistorted interference fringe.

The tilting of the beams in the intervals between exposures can be achieved by changing the positions of the mirrors or other optical elements of the experimental arrangement, but most conveniently, with the help of a thin refracting wedge introduced into the reference beam. In the intervals between exposures, the wedge is rotated⁷ or its index of refraction is changed.⁹ The direction and frequency of the reference fringes can be changed by changing the rotation angle, the wedge position and changing the position of the edge of the wedge relative to the reference beam. The frequency and direction of the reference fringes also can be changed by exposing the first and second holograms on different plates. By superposing the holograms, it is possible to achieve any frequency and direction of the reference fringes by shifting the holograms slightly.⁶⁸ This technique requires rather accurate matching of the holograms, and this gives rise to a number of technical difficulties.

4. STUDY OF PLASMAS

4.1. Laser sparks

A laser spark is formed when a powerful laser pulse is focused in air or some other gas. Results of studies of laser sparks carried out by various methods have been described in Ref. 69.

The holographic interferometry method provides the most complete information about this interesting phenomenon. An experimental apparatus designed for the study of laser sparks by the double-exposure holography method for time intervals of 40–200 ns⁷ (Fig. 12) consists of a ruby laser

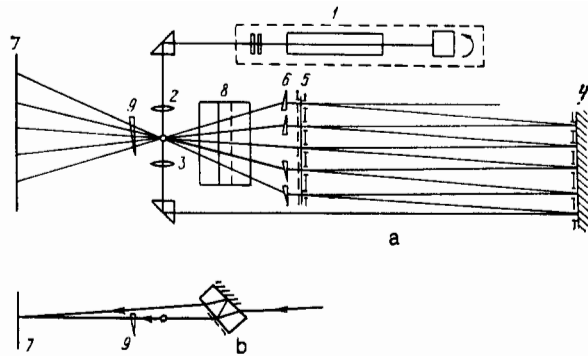


FIG. 12. Diagram of the experimental arrangement for the formation of cineholographic interferograms of laser sparks. a—Overhead view; b—side view.

1 whose Q -factor was modulated by a rotating prism. The laser beam passes through a telescopic system made up of lenses 2 and 3, at whose focal point a laser spark is formed. A rotating prism directs a collimated beam to the delay line that is formed by the regular and semitransparent mirrors 4 and 5, placed at a distance of 6.3 meters from each other, corresponding to a delay time of 42 nsec. A wedge 8, with a regular mirror on one side and a semitransparent mirror on the other side, is used to produce a reference beam. The angle and thickness of this wedge are chosen in such a way that the object and reference beams converge at the hologram plane⁷ at an angle of 1.5°. The diaphragms placed in front of the mirrors limit the beam diameters. The film is protected from exposure to radiation from the laser spark and scattered light by a red glass optical filter. In order to obtain double-exposure holograms, filters reducing the laser radiation below the breakdown threshold are introduced into the beam during the first exposure. In the interval between the first and second exposures a thin wedge 9 is rotated by a small angle around an axis perpendicular to the wedge plane. This leads to the appearance of the interferogram of reference fringes in the form of straight lines.

The duration of the laser pulse was about 30 ns. The trailing edge of the pulse is “cut off” by the plasma generated by the spark pulse. But this pulse duration is still too great for studying the initial stages of development of the spark. Interferograms of good quality were obtained only 80 nsec after the beginning of breakdown (see Fig. 14).⁷⁰ Although it is possible to draw some conclusions about the evolution dynamics of laser sparks from these interferograms, in order to obtain quantitative estimates of the sparks parameters it is necessary to separate the contributions of electronic and atomic components to the refraction index. With this aim in view further studies have been carried out by the methods of two-wavelength,^{71–74} dispersive⁷⁵ and resonance^{76,77} interferometry. In these articles, an apparatus was used with an optical delay line similar to the delay line described above. Light from a ruby laser model OGM-20 and also its second harmonic were used as the radiation source. A “home-made” pulsed dye laser has also been used for resonance interferometry. Most of the studies have been carried out for laser sparks in air; however, sparks in helium and hydrogen

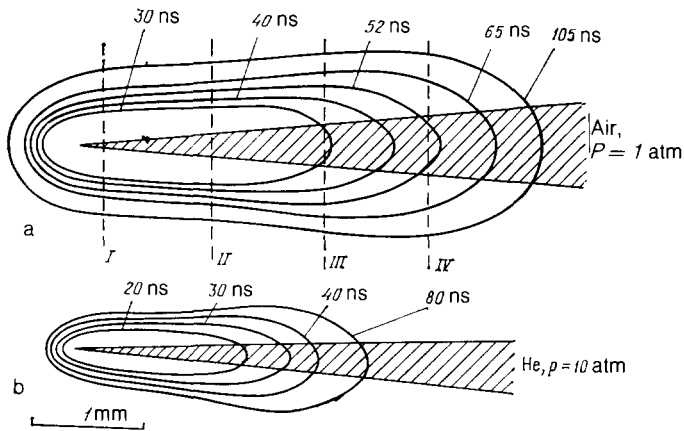


FIG. 13. Shape and dimension of a laser spark.

at different pressures (1–10 atm.) have also been studied.⁷³ Figure 13 shows the variation in the dimensions of a laser spark in air (a) and He (b); Fig. 14 shows an interferogram, and Fig. 15—the electron concentration distribution at different time instants.

An apparatus for forming two-wavelength holograms of focused images was developed.⁷⁴ For the reconstruction of the hologram an experimental arrangement was used that included a Mach-Zender interferometer which allowed one to vary the frequency and direction of interferogram fringes by adjusting the interferometer.⁷⁸ With the help of such an arrangement, it was possible to produce during the reconstruction of one two-wavelength hologram interferograms corresponding to each of the wavelengths present in the radiation, along with a dispersive interferogram. An analysis of the interferograms gives spatial distribution of electron concentrations and the air density in the spark. According to the

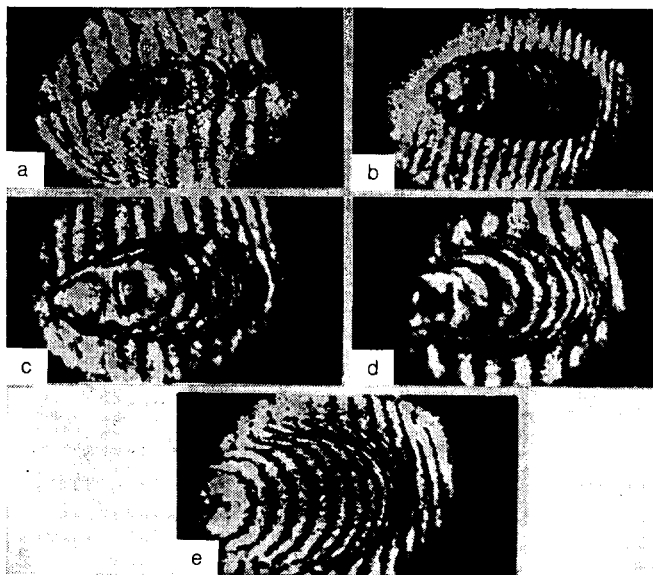


FIG. 14. Interferograms of a laser spark. Time (in ns) is measured from the beginning of a breakdown: 40 (a), 80 (b), 120 (c), 160 (d) and 200 (e). Photos a, b and c–e are obtained with different flashes.

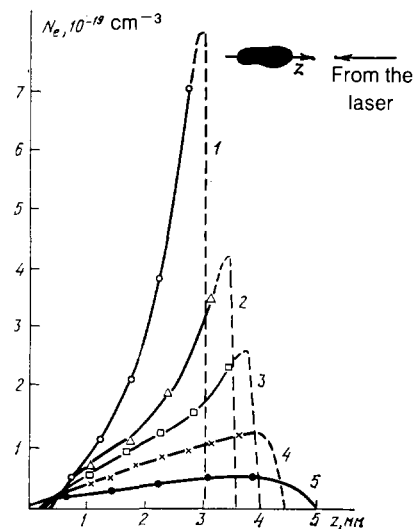


FIG. 15. Electron concentration distribution for different times ($P = 1$ atm).

authors, the error in determining N_e is approximately 4%. In Ref. 79 the later stages of laser spark evolution were studied with a CO_2 laser. The use of infrared radiation in this case is motivated by the desire to study this plasma at a moment when its electron concentration has decreased to the extent that studies with visible radiation are not sufficiently sensitive.

Laser sparks, including later stages of their evolution, have been studied also in Refs. 80–82. In order to form and transilluminate a spark, two lasers synchronized by a rotating prism that was modulating the Q -factor of both lasers were used in these papers. The laser used as a source of illumination generated two pulses with an interval of 200 nsec between them. The first pulse was generated before breakdown, the second—after the breakdown; as a result, a double-exposure hologram was produced during one laser burst. A double-pulse laser was used also for the study of laser sparks in helium in Ref. 83. In this work the electron concentration distributions were obtained from interferograms produced at different moments.

In Ref. 76 the method of resonance interferometry using a tunable dye laser has been used for the determination of the concentration of excited hydrogen atoms in a laser spark. Interferograms of a laser spark were obtained in the case when the illuminating radiation wavelength is close to the H_α line. Estimates of the sensitivity of resonance interferometry method were made taking into account the finite width of the absorption line. The method in which the interferograms produced with two different wavelengths are moiré superimposed has been used in order to increase the measurement accuracy of plasma dispersion. It was found that the electron concentration is approximately $(2-6) \cdot 10^{17} \text{ cm}^{-3}$ and the concentration of hydrogen atoms on the second energy level is $(4-6) \cdot 10^{14} \text{ cm}^{-3}$ in a laser spark plasma for an initial hydrogen pressure of 3 and 7 atm, and for the time instants 1–2 microseconds after the beginning of a breakdown.

The resonance absorption by a dye laser producing radiation with the wavelength equal to the wavelength of the H_{α} line, made it possible to obtain shadow projections of a laser spark in hydrogen and to investigate in detail the evolution of the shock wave caused by a laser spark over a large interval of pressures.⁷⁷ The results of the experiment were found to be in good agreement with the theory of a point explosion.

4.2. Laser jets

A plasma similar to the laser spark plasma but, usually, of higher density, is formed when laser radiation is focused on a solid state target. The study of such plasmas has been carried out by various methods, including the method of holographic interferometry.^{29,30,84-88}

In Refs. 29 and 87 are described the experimental apparatus and results of laser jet studies carried out by the resonance holography method for a potassium target. In order to produce three-wavelength holograms, the fundamental radiation of a ruby laser, its second harmonic and the stimulated Raman scattering of the fundamental frequency by nitrobenzene were used. The wavelength of the fundamental radiation ($\lambda = 865.8$ nm) differs only by 0.7 nm from the wavelength of the resonance line of KI. This fact allows one to increase the sensitivity with which the concentration of potassium atoms was determined by two orders of magnitude compared to the sensitivity that can be obtained by using radiation far from the absorption line. The use of three-wavelength holograms made it possible to find independently the concentration of electrons, potassium atoms and air molecules. In Fig. 16 these results are shown for a time instant 115 nsec after the beginning of breakdown. The lowest value of IN that can be detected under these conditions is estimated to be around $\approx 10^{14}$ cm⁻².

In Ref. 88 the measurement of lithium atom concentrations was carried out by the resonance interferometry method using a dye laser. The experimental apparatus consisted of two lasers; one was a neodymium glass laser, whose radiation was focused on the Pb-Li alloy to produce jets, and a ruby laser which was used to form the hologram. Both neodymium and ruby lasers were modulated by a rotating prism in such a way that it was possible to vary the time interval between pulses in the range 0.3–2.5 μ sec by changing the position of a modulating prism relative to the lasers.

The second harmonic of the ruby laser pumped a cell with a dye solution, that was placed in the resonator to achieve wavelength selection. The dye generated a single line

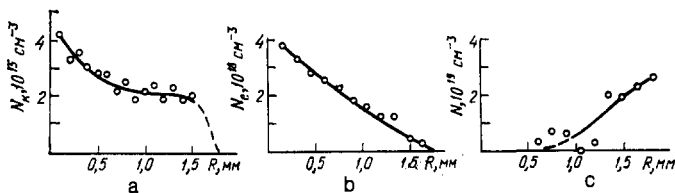


FIG. 16. Radial concentration distribution along the jet cross-section ($\tau_{del} = 115$ nsec after beginning of a breakdown).³³ a—Potassium atoms, b—electrons, c—air molecules.

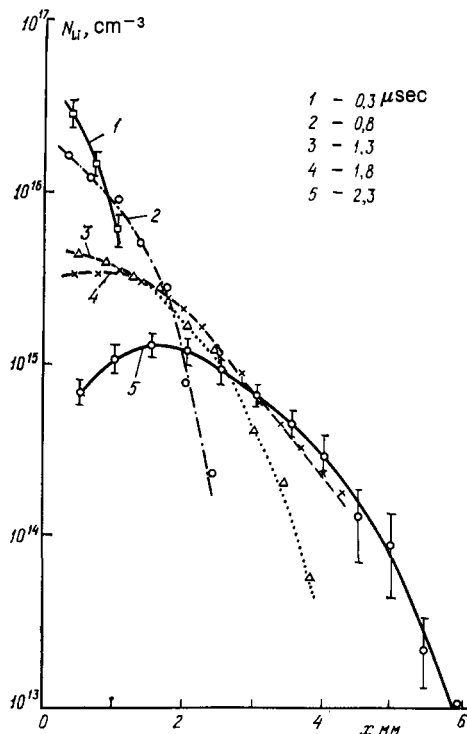


FIG. 17. Lithium atom concentration for different distances from a target. Time from the moment of a jet formation in μ sec: 0.3 (1), 0.8 (2), 1.3 (3), 1.8 (4), 2.3 (5).

with a width of 0.05 nm, whose position relative to the lithium absorption lines ($\text{Li} = 670.77$ and 670.79 nm) could be changed in such a way that the sensitivity of the measurements would be maximal.

Both the radiation of the dye laser and the main radiation of the ruby laser have been used to form interferograms. The data on the lithium atom concentration along the laser beam axis for different time instants from the beginning of the jet formation are given in Fig. 17.⁸⁸

For each region of concentration variation a corresponding $\lambda - \lambda_0$ value was chosen; λ is the wavelength of the probing laser line, λ_0 is the wavelength of the sodium resonance. This made it possible to include the concentrations of N_{Li} from 10^{13} to 10^{17} cm⁻³. It should be noted that the concentration of lithium atoms at a distance of 2–3 mm from the target remains almost constant during the entire observation time.

Resonance holography was also used for measuring the BaII ion concentration in a plasma generated by a CO₂ laser which was focused on a barium target placed in a vacuum chamber.⁸⁹ Interferograms were produced using a pulsed dye laser with a narrow emission line that was selected to be close to the BaII resonance line with $\lambda = 454.4$ nm. The barium ion concentration could be measured for values less than $5 \cdot 10^{13}$ cm⁻³. In this work, information which was known already at least 5–7 years earlier was rediscovered by resonance holography (see, e.g., Refs. 29–30).

In the last several years special attention has been given to investigating plasmas related to studies of laser-induced thermonuclear fission. The typical plasma parameters for

this case are: linear dimensions of 10–100 μ , electron density of $\approx 10^{21} - 10^{22} \text{ cm}^{-3}$, speeds of separation— $10^6 - 10^7 \text{ cm} \cdot \text{sec}^{-1}$, and times $\sim 10 \text{ psec}$.

Optical studies of plasmas with such parameters require extremely precise experimental techniques, and have become possible only with the development of picosecond lasers. Many papers are devoted to this subject (see, e.g., Ref. 90). Here we consider only the papers which mainly use holographic interferometry.

A plasma formed near an aluminum surface during the irradiation of the surface by picosecond pulses of a neodymium laser was studied in Ref. 86. The second harmonic of the same laser was used as a source of probing radiation. An extremely high temporal resolution of $7 \cdot 10^{-12} \text{ sec}$ has been achieved.

Subsequently, research techniques were continuously improved in a series of articles^{91–96}; some of the results of these articles are given below. As a rule, a plasma with the required parameters can be created by a neodymium laser pulse with a power of several terawatts and pulse length of 100 ps striking a spherical target whose size was $\sim 100 \mu$.⁹⁴ The electron density of the plasma formed in this way is not more than 10^{22} cm^{-3} in the first instants after its formation; at the same time, the critical density above which radiation with a wavelength of $\lambda = 1.06 \mu$ does not penetrate into the plasma is $1.0 \cdot 10^{21} \text{ cm}^{-3}$. For another wavelength we have

$$N_{e \text{ crit}} = 1.0 \cdot 10^{21} \left[\frac{1.06 \mu}{\lambda (\mu)} \right]^2.$$

Thus, when working with high density plasmas it is necessary to decrease the wavelength of the probing radiation.

In the beginning this was done by frequency-doubling ($\lambda = 503 \text{ nm}$) in a nonlinear crystal, then by frequency-tripling ($\lambda = 353 \text{ nm}$).⁹² In later work the fourth harmonic of a neodymium laser was used, which was obtained by repeated doubling of neodymium laser fundamental frequency in KDP and ADP crystals.⁹⁴

As an example we give experimental data obtained in this latter paper. Glass spheres of $\sim 40 \mu$ in diameter were illuminated by a laser pulse ($\lambda = 1.06 \mu$, $\tau = 30 \text{ ps}$). A small portion of the pulse energy was separated from the main beam by the beam-splitter 1 (Fig. 18), which after traversing the KDP and ADP crystals and the optical filter 2 (which passed only ultraviolet probing radiation) passed through the plasma. (The duration of the probing pulse was less than 15 ps.) The plasma was formed in the vacuum chamber 3 with quartz windows and lenses.

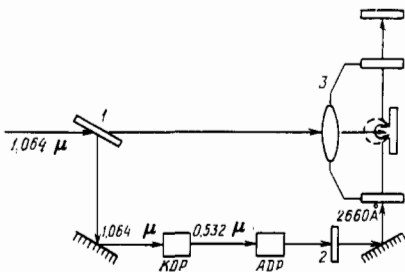


FIG. 18. Ultraviolet interferometry of plasma.

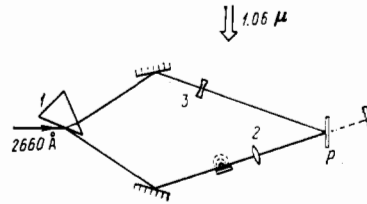


FIG. 19. Ultraviolet holographic microinterferometer.

Holograms were formed by a holographic micro-interferometer, a sketch of which is given in Fig. 19. Before reaching the chamber, the probing beam was split by the quartz prism 1 into two beams of nearly equal intensity following symmetrical paths. The object beam was widened by the microobjective 2, and the reference beam by the lens 3. The hologram was photographed in the plane *P*. Interferograms were formed by the double-exposure method. Very precise focusing of the microobjective is essential for obtaining holograms of good quality: a focusing error of 40 μ leads to a substantial variation of the number of fringes on an interferogram.

The problem of focusing was studied in more detail in Refs. 97, 98. In Ref. 97 the influence of focusing on the measurement of N_e (in the range $10^{17} - 10^{18} \text{ cm}^{-3}$) in a plasma formed by the action of a focused neodymium laser on the end face of a carbon filament $\sim 10 \mu$ in diameter (the power of the laser is 100 GW, $\tau = 20 \text{ ps}$, target illumination is $3 \cdot 10^{18} \text{ W/cm}^2$). A probing beam is obtained by using the fourth harmonic of the same radiation (whose beam energy is about $10 \mu\text{J}$, $\tau \approx 10 - 15 \text{ ps}$). The microobjective formed a plasma image in the hologram plane. This is how the holograms of the focused images were formed in these and other papers described above. It has been shown that for correct measurements of N_e the microinterferometer focusing error should not exceed 5 μ . An error of over 40 μ amounts to more than 100% deviation from the actual value of N_e . This fact allowed the authors of Ref. 98 to suggest a new holographic method for measuring the electron concentration near its critical value. In this method beams falling on the plasma at some angle to its surface undergo a significant deflection which leads to a shift of the interference fringes in the reconstructed interferogram.

This makes it possible, by varying the focusing conditions for a plasma image at the stage of reconstructing the hologram and measuring the distances between rings for different focusing conditions to obtain a radial distribution of N_e . It is interesting to note that this method, unlike the conventional holographic interference methods, does not require the use of the Abel method for interferogram analysis.

Reference 98 also gives the results of N_e measurements in the $(1-3) \cdot 10^{21} \text{ cm}^{-3}$ region out to a distance of 5–20 μ from the center. The measurements were carried out both by the conventional and new methods, and are in very good agreement with each other.

4.3. Neutral current layers

Interest in the study of neutral current layers formed in plasmas near the zero line of a magnetic field is related main-

ly to studies of cosmic plasmas. Such layers are formed in high-current discharges placed in a magnetic field with a specially chosen configuration. A number of holographic studies of this phenomenon, which were carried out on the experimental system TS-3, have made it possible not only to visualize the neutral layer clearly but also to carry out measurements of the electron concentration distribution along the two axes perpendicular to the current direction.

The diameter of the installation discharge chamber is 10 cm, the distance between electrodes is about 80 cm. Discharge currents up to 50 kA were achieved. It is obvious that for an installation with these parameters, the use of interferometric methods other than holographic interferometry is practically unrealistic. In the first work in which this phenomenon was investigated, measurements were made by the double-exposure holographic interferometry method.

For each current pulse through the chamber one interferogram was produced; insufficient reproducibility of the discharge pulses made it impossible to observe the dynamics of the current layer. For this reason, in subsequent papers¹⁰⁰⁻¹⁰² a five-frame cineholographic installation was constructed, whose schematic diagram is given in Fig. 20. It differs from the one-pass system described in Ref. 99 in that the beam 1, which comes from the OGM-20 laser and is expanded by the telescopic system 2, after passing the delay line 3, the system of semitransparent mirrors 4 and the telescopic system 5 which expanded the beam diameter up to 7 cm (the diameter of the discharge chamber window), was used to form five aligned beams delayed relative to each other by 60 ns. These beams passed along the axis of the chamber 6, were narrowed down to a diameter of about 20 mm by the telescopic system 7 and reached the transparent grating 8 (150 lines/mm) which split the aligned beams into five beams at the grating angles relative to each other (0^{th} , ± 1 and ± 2 -orders). These beams formed five separate images in the hologram plane 9. Before they passed through the plasma, the laser beams delayed by the line 3 were directed by the semitransparent mirror 10 to the mirror 11 and after they passed the telescopic system 12, each beam was aligned

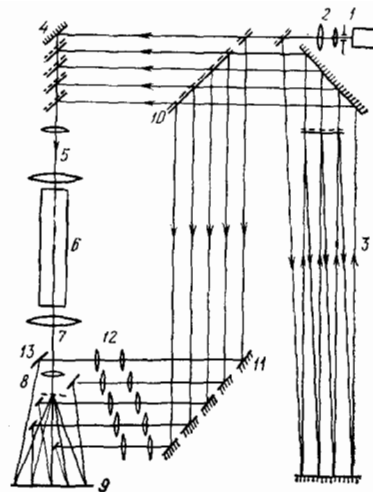


FIG. 20. Simplified diagram of a cineholographic installation (cf. Ref. 102).

with one of the images in the hologram plane by its mirror from the mirror group 13. Only beams which traveled equal distances through the delay line could be interfering.

Thus, each of the five holograms received an additional noncoherent exposure from the four object beams, whose delays were different from the delay of the reference beam. Five-frame interferograms were produced by this installation (Fig. 21). The time interval between two frames was 60 ns, and the laser pulse duration was 30 ns. The two-dimensional distribution of electron concentration across the discharge axis as determined from the interferograms 1, 3, and 5, is shown in Fig. 22. In all the measurements it was assumed that the electron concentration along the discharge axis was constant.

4.4. z- and θ -pinches

Holographic studies of plasmas in large installations for thermonuclear fission have been carried out in a number of papers by Soviet^{103,105} and foreign researchers.^{9,106-110} In

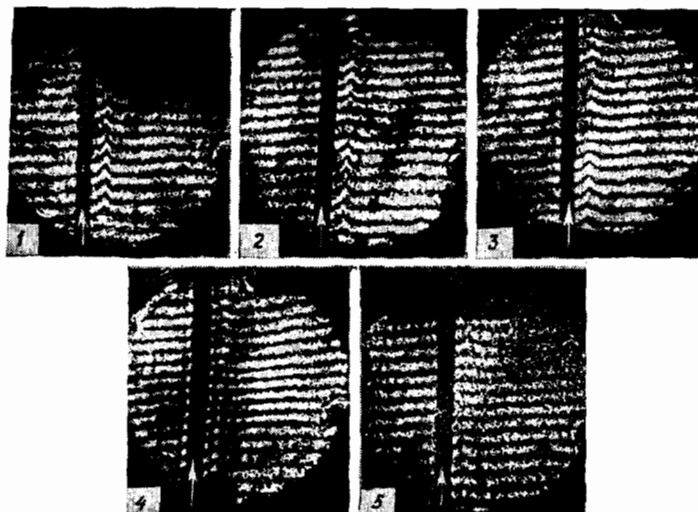


FIG. 21. A five-frame interferogram series obtained 1.5 μsec after the beginning of a discharge (arrows indicate probe shadows).

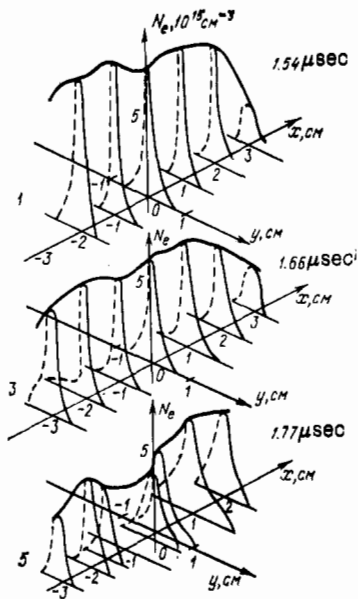


FIG. 22. Electron concentration distribution obtained from the interferograms of Fig. 21 (interferograms 1, 3 and 5).

Refs. 103, 104 the θ -pinch was studied in a discharge chamber with a length of 1 meter and a probing beam diameter of 10 cm. The laser used was a single-mode ruby laser (with a coherence length of approximately 1 meter) with an electro-acoustic Q -switch, the switching on moment of which could be made to coincide with the required stage of the discharge. A θ -pinch with a length of three meters was studied in Refs. 108, 109. In these papers also the modulation of the ruby laser was accomplished with an electro-optic shutter, synchronized with a particular phase of the discharge. In order to obtain cineholograms of the later plasma development stages, the plasma was illuminated by three lasers, which emitted at intervals shifted by $2 \mu\text{sec}$ relative to each other. The object beams from all three lasers were made to traverse the same path along the chamber axis with the help of a system of semitransparent mirrors. A grating placed at the exit from the chamber divided the exiting beam into three beams (0- and ± 1 orders) that formed three spatially separated interferograms corresponding to different development stages of the discharge.

The use of two synchronized lasers was described already in the first works on the study of the θ -pinch in the installation "Scilla."^{106,107} In these papers very good holograms of focused images with the use of frosted glass as the scatterer have been obtained. Unlike the approach in most papers, in which, in order to form linear reference fringes on the interferogram, a wedge or one of the mirrors was rotated during intervals between exposures, thus changing the angle between the reference and object beams, in Refs. 106, 107 a prism-shaped cell filled with SF_6 was placed in the object beams for this purpose. Variation of the gas pressure or substitution of the SF_6 by air led to the required change of beam tilt.

Later holographic interferometry was used for electron concentration determination at different stages of the θ -

pinch.¹¹⁰ Plasma was illuminated perpendicular to the discharge axis by a Nd:YAG laser (the duration of the pulse is 5 ns). A radial distribution of N_e was obtained by using the Abel inversion method for the analysis of holographic interferograms. The diameter of the plasma channel was 2 mm during the maximal compression, and the maximal density along the discharge axis was $N_e = 1.5 \cdot 10^{18} \text{ cm}^{-3}$.

4.5. Flash lamp plasmas

Flash lamps for the optical pumping of solid-state and liquid lasers and for other applications were studied by methods of holographic interferometry in Ref. 8. Quartz tubes of such lamps contain many strias and other inhomogeneities, and this requires the use of lasers with good spatial and temporal coherence for their investigation. A single-pulse ruby laser was used for this purpose in Ref. 8. Selection of transverse modes was achieved with the help of a diaphragm placed into the resonator. However, this reduced the energy of the beam to such an extent that the exposure of a hologram to the radiation from the plasma significantly decreased the quality of the interferograms, and as a result, quantitative measurements were difficult to perform. Interferograms of significantly better quality have been obtained in Refs. 111, 112, in which plasma was illuminated by a single-mode ruby laser with an optical amplifier. To suppress the exposure of the hologram to the lamp radiation, the photographic plate was covered by an interference filter with a narrow band-pass near $\lambda = 694.3 \text{ nm}$. Despite this measure, the parasitic radiation of the lamp significantly reduced the quality of the interferograms. Deformations of the lamp walls, that occur during a pulse and that are caused both by shock waves and by a thermal mechanism, can have some influence on the position of interference fringes.

4.6. CO_2 laser-induced plasmas

One of the obstacles delaying the development of infrared holography is an insufficiently high coherence of the radiation from CO_2 -pulsed lasers. This insufficiency is caused by the inhomogeneities of the active media in CO_2 -lasers that arise as a result of nonuniform heating of the gas by a discharge pulse. Such inhomogeneities have different magnitude and structure depending on the design of the discharge tube, electrodes, gas pressure, pumping rate, etc.

The most complete information about the character of these inhomogeneities and methods for reducing them can be obtained by methods of holographic interferometry that have been used for this purpose in a series of papers of Refs. 113, 119. It was established that the refractive index of a CO_2 laser plasma is determined only by the refractive index of the working gas, and that the electron component of the plasma gives a negligibly small contribution to it. The same is true for most types of plasmas that will be considered later.

An experimental apparatus for interference-holographic investigations of CO_2 lasers that is described in Refs. 113–115 had several modifications. The schematic diagram of one of them is shown in Fig. 23. A beam from a ruby laser (energy of radiation is 0.01 J, the pulse duration is $\approx 40 \text{ ns}$, the coherence length is $L > 3 \text{ m}$) was expanded by the tele-

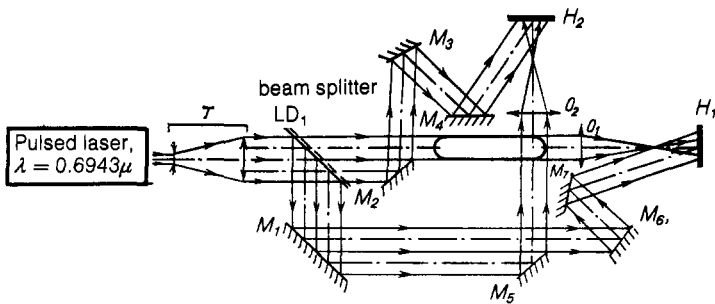


FIG. 23. Installation for the study of CO₂-lasers.

scope T and directed to the beam-splitting mirror LD_1 . The beam reflected from this mirror was rotated by the mirror M_1 and was divided into two beams by the mirrors M_2 and M_6 . The mirror M_7 rotated the part of the beam that served as the reference beam for the hologram H_1 . Another part of

the same beam illuminated the CO₂ laser in the direction perpendicular to the discharge axis, and served as the object beam for the hologram M_2 . The almost symmetrical system of the mirrors M_2 , M_3 , and M_4 gave rise to the reference beam for the hologram H_2 and the object beam for the hologram H_1 .

Figure 24a shows one of a series of interferograms, and Fig. 24b shows the spatial distribution of a gas mixture density calculated for the time $20 \mu\text{sec}$.¹¹⁴ The dynamics of shock wave propagation, gas heating, local density fluctuations near electrodes, etc., have also been studied. This work made it possible to select optimal conditions for obtaining the most coherent radiation for pulsed CO₂ lasers.

4.7. Plasmotrons

The first work on the study of plasmotrons dealt with a plasma jet generated in a constant current plasmotron with vortex-type stabilization and a power of 3 Kw ($I = 25 \text{ A}$, $U = 120 \text{ V}$). Two-wavelength holography with the fundamental and second harmonic of the ruby laser radiation was used. From the analysis of the interferograms it was found that $N_e < 10^{17} \text{ cm}^{-3}$ and that the fringe shifts are caused only by a gas density decrease in the plasma region.¹²⁰ In Ref. 121 a pulsed plasmotron was studied in real time. For this purpose, one of two holograms that were used to form an interferogram (without the plasmotron) was photographed on a photographic plate, which was then developed and processed without being moved from its original position, so as not to shift the formed image. Holograms of the plasma were produced by using a ruby laser that worked in the multimode regime with the pulse duration $\approx 1 \mu\text{sec}$.

In this way, a series of plasma holograms was formed in the plane of the developed hologram. An interferogram of the plasma jet obtained by superposing these holograms was photographed by a high-speed streak camera working in the gated image mode. The time between frames was measured from the distance between them and was approximately several tens of microseconds. A similar approach using an electron-optical converter was taken in Ref. 122 for the study of spark breakdown.

A detailed study of the behavior of a plasmotron jet was carried out in Ref. 123. A holographic interferometer used in this work allowed one to perform the study by the double-exposure method and in real time. The conditions for the transition of laminar flow of a plasma jet into turbulent flow have been studied. The temperature distribution along the plasma jet radius and jet pulsations in different plasmotron

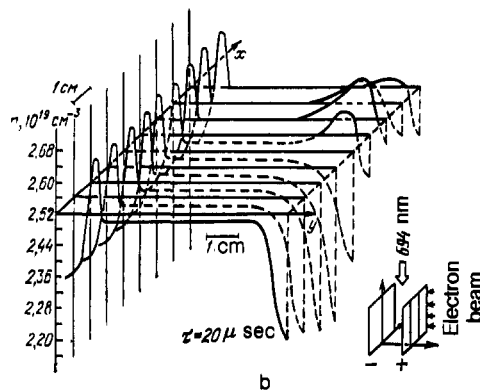
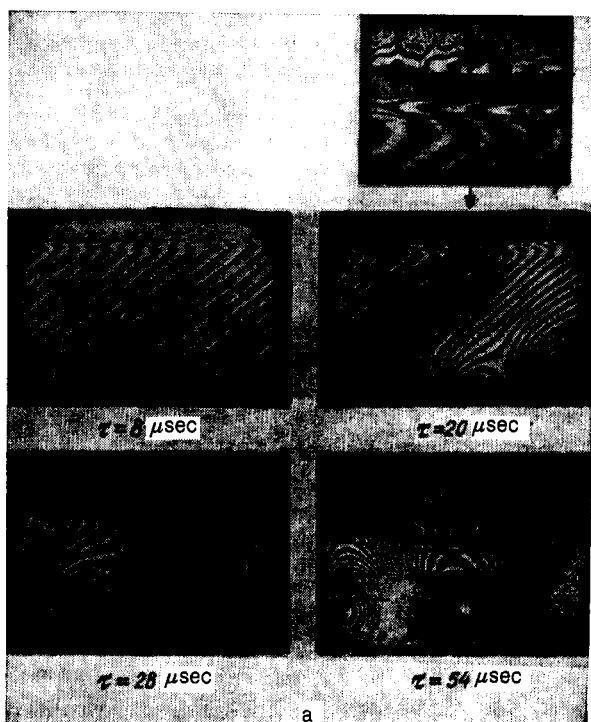


FIG. 24. a—Interferograms of the discharge in a CO₂ laser; the magnified region near electrodes is shown in the upper right corner. b—Gas density distribution in a CO₂ laser.

modes were found from the shift of interference fringes by using the known temperature dependence of the refractive index of nitrogen (the working gas of the plasmotron).

Two wavelength holographic interferometry has been also used for studying the plasma of the laser plasmotron, i.e., the stationary plasma formed by the continuous radiation of a powerful CO₂-laser.¹²⁴ The electron concentration distribution was measured in the plasma formed by a 6.2 kW laser in N₂ at atmospheric pressure.¹²⁵

A laser plasmotron was studied also in Ref. 126, where the radial temperature distribution in an argon plasma was investigated. In the central region of the plasma, where the temperature reaches its peak, the temperature was determined by a spectroscopic method, and in the colder areas—by a holographic method. The holographic method was also used to measure the distribution of refractive index, from which it was possible to calculate the temperatures of the various regions of the plasma. A study of a plasma jet was done also with a pulsed HF-laser having the emission lines near $\lambda = 3 \mu$. The CO₂ laser could not be used in this case since its radiation (10.6 μ) is absorbed by the quartz walls of the cell.⁵⁴

4.8. Exploding conductors

When a powerful current pulse is passed through a thin conducting wire, the wire can explode, forming a plasma. Such plasmas have been studied by various methods, including the holographic interferometry method. In Ref. 127 the original method of forming two-wavelength holograms was used for this purpose. The idea of the method is clear from Fig. 25, which shows the optical scheme of the experiment. The light beam containing the fundamental and second harmonic (λ_1 and λ_2) wavelengths of the pulsed ruby laser radiation is split by the semitransparent mirror 1 into two beams, one of which is used to form the object beam, which then passed through the plasma formed by the wire *O*. Another beam was divided by the beam splitter 2 into two reference beams, from which the optical filters *F*₁ and *F*₂ selected radiation with the wavelengths λ_1 and λ_2 , respectively. These two beams illuminated two different areas of the hologram *H*. The object beam, after it passed the diffuser *R*, illuminated the entire hologram *H*.

In this way, the two holograms formed by the radiation with the wavelength λ_1 and λ_2 were recorded simultaneously in the plane *H*.

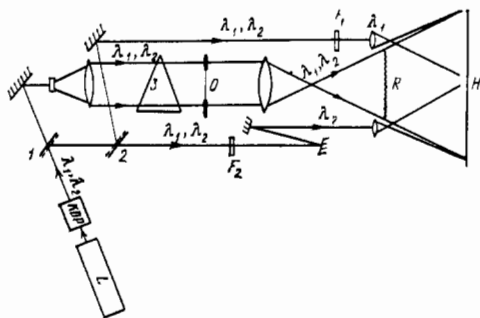


FIG. 25. An installation for the study of plasma of exploding conductors.

By changing the pressure in the gas-filled prism 3, placed in the object beam, it was possible to obtain rectilinear reference fringes. From the analysis of both interferograms it was possible to find separately the refractive indices of the atomic and electron gases. A similar study has been carried out in Ref. 128.

4.9. Electric arcs and other types of discharges

High-current arcs were studied in Refs. 129–130. Holograms in this case were formed by the usual two-exposure method. A chamber with a gas flow, in which a powerful arc was burning between two electrodes (the current is 1850 A), was placed in the object beam. A narrow-band interference filter, when the hologram is at a sufficiently great distance from the filter, completely suppressed the disturbances created by the arc radiation. From the interferograms obtained in this way it was possible to measure the radial temperature distribution in the arc.

Asymmetric plasma in an argon cascade arc, placed in a magnetic field, was studied in Ref. 131. For this purpose, seven laser beams, lying in the plane perpendicular to the discharge axis and tilted relative to each other at the angle 15°, illuminated the discharge column. All these beams were formed by splitting one laser beam that diverged within limits of 90°. By analyzing seven interferograms, it was possible to obtain refractive index distribution, and from it to find the radial temperature distribution.

Electrical breakdown of air was studied by the cineholographic method in Ref. 32.

Discharge of a capacitor ($V = 30$ kV; $C = 0.04 \mu\text{F}$) was studied in Ref. 133. Two-exposure holograms were formed when a probing ruby laser beam passed along the axis of the discharge channel initiated by a CO₂ laser. A discharge took place 5 μsec after the end of a laser pulse, and it was possible to vary the beginning of the probing pulse to be 30–70 μsec after the beginning of the discharge. Discharge experiments were done in He, Ar and other gases. The formation and propagation of shock waves and other gasodynamic phenomena have been studied.

The plasmas in the self-sustained and non-self-sustained discharges in weakly ionized molecular gases (argon and CO₂-N₂-He mixtures) were studied by holographic interference methods in Refs. 134–136 for the case of pulsed periodic discharges. The propagation of shock waves, development of “streamers,” the distribution of temperature and velocities in a gas flow, and the character and magnitude of gasodynamic perturbations have been studied. All this work, as well as the work in Refs. 113, 119, was done in connection with the study of processes taking place in the CO₂ laser plasmas.

A low voltage pulsed arc discharge in cesium vapor ($p = 1$ tor, $I = 50$ A) was studied in Ref. 137. By using the resonance holography method with a dye laser, which was generating the line separated by 0.06–0.1 nm from the short-wave component of the main series doublet (CsI $\lambda = 455.5$ nm), it was possible to obtain the radial distribution of cesium atom and ion concentrations for different densities of the arc current.

In Refs. 138–139 a new resonance holography method

was suggested and realized, which was applied for determination of the concentration of calcium atoms in a hollow cathode plasma. For this purpose an isotopic shift between ^{40}CaI and ^{48}CaI was used, which is 0.05 cm^{-1} (0.01 \AA) for the resonance line $\text{CaI } \lambda = 422.7\text{ nm}$. The atom concentration in a hollow cathode, containing calcium with the natural isotope content of 97% of ^{40}Ca was measured. A second gas-discharge tube with a hollow cathode contained calcium enriched in the heavy isotope (68% ^{48}Ca , 30% ^{40}Ca). The radiation from this tube (cooled by liquid nitrogen) illuminated the plasma of a ^{40}Ca vapor discharge, and formed a holographic interferogram in the plane of the wide slit of the spectrograph. In the focal plane of this device a series of interferograms were formed, corresponding to different lines emitted by the hollow cathode, but only one line, corresponding to the resonance line, was used. Due to the very narrow plasma absorption and emission lines, the sensitivity for atomic concentration determination was much higher than in other papers ($N\lambda \sim 2 \cdot 10^{11}\text{ cm}^{-2}$ instead of approximately $3 \cdot 10^{12}\text{ cm}^{-2}$, as follows from the graph in Fig. 5, for which $N\lambda$ was calculated for the maximum approach to the line center of 0.1 \AA). The experimental conditions for a hollow-cathode plasma make it possible to approach λ_0 at least ten times closer than in plasmas investigated in other papers on resonance holography. Thus, the achieved low concentrations are in agreement with the calculations made in Refs. 31, 32 and the experiments described above (see, for example, Refs. 32, 33).

Spectral analysis makes it possible, in principle, to measure simultaneously, by the proposed method the concentrations of atoms of several elements by using the many-element hollow cathodes with various isotope composition. However, so far this approach has not been realized.

The glow discharge in xenon was studied in Ref. 140 for a pressure of several tor. The radial temperature distribution in the discharge column has been obtained from holographic interferograms.

The author is very grateful to G. V. Ostrovskaya and Yu. I. Ostrovskii for useful discussions and for providing a number of figures, photographs and other materials.

After this article was submitted for publication A. M. Prokhorov, N. V. Karlov and their co-workers have published a number of papers describing the holographic interferometry studies of optical discharges in pure gases and near solid targets.¹⁴¹⁻¹⁴⁵

The discharges were excited by powerful CO_2 lasers for the argon and helium pressures in the range from 5 to 100 mm Hg.¹⁴² The speed of propagation of shock waves, ionization waves and other gasdynamic processes have been determined from holographic interferograms.

The experiments on the focusing of radiation on a solid Al target were done with a laser with an unstable resonator.¹⁴⁴ A spherical mirror focused radiation into a ring-shaped spot, with the power density in the range 1-16 Gwt/cm². The maximal amount of energy incident on the target was 400 J.

Interferograms in all the papers mentioned above were formed by a OGM-20 ruby laser, the pulses of which were

synchronized within 20 ns with the CO_2 laser pulses, having a pulse half-width of 100 ns.

Excellent holographic interferograms have allowed the measurement of the radial distribution of electron density at several cross sections of a tube-shaped plasmoid (the length $\approx 2\text{ cm}$, the diameter $\approx 0.5\text{ cm}$) and to study the process of its collapse.

A jet formed by CO_2 laser irradiation of a copper target has been studied in a similar method in Ref. 146.

¹¹Recently the construction of an interferometer was reported in which the infrared probing wave ($5.23\text{ }\mu$) after passing through the plasma was converted to the visible region ($0.613\text{ }\mu$) by mixing with the radiation from a ruby laser ($0.694\text{ }\mu$) in a LiI crystal.^{17c}

¹Yu. I. Ostrovskii, M. M. Butusov, and G. V. Ostrovskaya, *Golograficheskaya interferometriya*, Nauka, M., 1977 [Engl. Transl., *Interferometry by holography*, Springer-Verlag, Heidelberg-New York, 1980] (Springer series in optical sciences: V. 20).

²C. M. Vest, *Holographic interferometry*, Wiley, New York, 1979. [Russ. Transl., Mir, M., 1982].

³W. Schumann and M. Dubas, *Holographic interferometry: from the scope of deformation analysis of opaque bodies*, Springer-Verlag, Berlin, 1979 [Russ. Transl., Mashinostroenie, L., 1983].

⁴*Golograficheskaya interferometriya fazovikh ob'ektov* (Holographic interferometry of phase objects), Ed. G. I. Mishin, Nauka, Leningrad, 1979.

⁵G. Wernicke and W. Osten, *Holografische Interferometrie*, VEB Fachbuchverlag, Leipzig, 1982.

⁶R. J. Collier, C. B. Burckhardt, and L. H. Lin, *Optical holography*, Academic Press, N. Y., 1971 [Russ. Transl., Mir, M., 1973].

⁷A. Kakos, G. V. Ostrovskaya, Yu. I. Ostrovsky, and A. N. Zaidel, *Phys. Lett.* **23**, 81 (1966).

⁸Yu. V. Ashcheulov, A. D. Dymnikov, Yu. I. Ostrovsky, and A. N. Zaidel, *Phys. Lett.* **A24**, 61 (1966).

⁹F. C. Jahoda, R. A. Jeffries, and G. A. Sawyer, *Appl. Opt.* **6**, 1407 (1967).

¹⁰F. S. Jahoda, 8th Intern. Conference on Phenomena in Ionized Gases, Vienna, 1967, p. 508.

¹¹A. N. Zaidel', G. V. Ostrovskaya, and Yu. I. Ostrovskii, *Zhurn. Tekh. Fiz.* **38**, 1406 (1968) [Sov. Phys. Tech. Phys. **13**, 1153 (1969)].

¹²A. N. Zaidel', G. V. Ostrovskaya, and Yu. I. Ostrovskii, *Trudy GOI* (Proceedings of the State Institute of Applied Optics), **42**, 23 (1975).

¹³A. N. Zaidel' and G. V. Ostrovskaya, *Lazernye metody issledovaniya plazmy* (Laser methods of plasma research), Nauka, Leningrad, 1977.

¹⁴G. V. Ostrovskaya and Yu. I. Ostrovsky, *Prog. Opt.* **22**, 197 (1985).

¹⁵A. B. Berezin, I. I. Komissarova, G. V. Ostrovskaya *et al.*, *Zh. Tekh. Fiz.* **52**, 1432 (1982) [Sov. Phys. Tech. Phys. **27**, 873 (1982)].

¹⁶I. Ursu, D. Apostol, I. Apostol *et al.*, *Zh. Tekh. Fiz.* **52**, 1432 (1982) [Sov. Phys. Tech. Phys. **27**, 873 (1982)].

¹⁷a) I. I. Komissarova, G. V. Ostrovskaya, Yu. I. Ostrovsky *et al.*, XVII Intern. Conference on Ionized Gases, Budapest, 1985, p. 1099. b) P. A. Bagryanskiĭ, A. A. Baksheev, and V. S. Balkin, Proceedings of the 3rd All-Union Meeting on High Temperature Plasma Diagnostics, JINR, Dubna, 1983, p. 129. c) Yu. M. Gorbunov, D. M. Zlotnikov, and I. A. Znamenskaya, *ibid.*

¹⁸G. V. Ostrovskaya, Trans. of Intern. Conference and School "Lasers and Applications," Bucharest, 1982, p. 302.

¹⁹G. V. Ostrovskaya, Proc. 3rd Intern. Conference on Infrared Physics, Zurich, 1984, p. 133.

²⁰V. E. Golant, A. P. Zhilinsky, and S. A. Sakharov, *Osnovy fiziki plazmy*, Atomizdat, M., 1977 [Engl. Transl. *Fundamentals of plasma physics*, Wiley, N. Y., 1980].

²¹O. M. Fridrich, F. Weigel, and A. A. Dougal, *IEEE J. Quantum Electron.* **QE-5**, 360 (1969).

²²F. Weigel, O. M. Fridrich, and A. A. Dougal, *ibid.* **QE-6**, 41.

²³I. I. Komissarova, G. V. Ostrovskaya, V. N. Filippov, and E. N. Shedova, *Zh. Tekh. Fiz.* **53**, 251 (1983) [Sov. Phys. Tech. Phys. **28**, 156 (1983)].

- ²⁴O. Bryngdahl and A. W. Lohmann, *J. Opt. Soc. Am.* **58**, 141 (1968).
- ²⁵K. S. Mustafin, V. A. Seleznev, and E. I. Styrkov, *Opt. Spektrosk.* **28**, 1186 (1970) [*Opt. Spectrosc.* (USSR) **28**, 638 (1970)].
- ²⁶K. Matsumoto and M. Takashima, *J. Opt. Soc. Am.* **60**, 30 (1970).
- ²⁷A. F. Belozarov, K. S. Mustafin, A. I. Sadykova *et al.*, *Opt. Spektrosk.* **29**, 384 (1970) [*Opt. Spectrosc.* (USSR) **29**, 204 (1970)].
- ²⁸A. F. Belozarov, A. N. Berezkin, L. T. Mustafina *et al.*, *Fizicheskiye issledovaniya prozrachnykh neodnorodnostei* (Physics of Transparent Inhomogeneities, MDNTP, M., 1977, p. 45).
- ²⁹G. V. Dreiden, Yu. I. Ostrovsky, E. N. Shedova, and A. N. Zaidel, *Opt. Commun.* **4**, 209 (1971).
- ³⁰G. V. Dreiden, A. N. Zaidel', Yu. I. Ostrovskii, and E. N. Shedova, *Zh. Tekh. Fiz.* **43**, 1537 (1973) [*Sov. Phys. Tech. Phys.* **18**, 972 (1974)].
- ³¹B. M. Measures, *Appl. Opt.* **9**, 737 (1970).
- ³²G. V. Dreiden, A. N. Zaidel', G. V. Ostrovskaya *et al.*, *Fiz. Plasmy* **1**, 462 (1975) [*Sov. J. Plasma Phys.* **1**, 256 (1975)].
- ³³D. V. Dreiden and E. N. Shedova, *Opticheskaya golografiya* (Optical holography), Ed. Yu. I. Ostrovskii, Nauka, Leningrad, 1975, p. 71.
- ³⁴R. A. Alfer and D. R. Wite, *Phys. Fluids* **1**, 452 (1958); **2**, 153, 162 (1959).
- ³⁵R. W. Meier, *J. Opt. Soc. Am.* **56**, 219 (1966).
- ³⁶G. V. Ostrovskaya and Yu. I. Ostrovskii, *Zh. Tekh. Fiz.* **40**, 2419 (1970) [*Sov. Phys. Tech. Phys.* **15**, 1890 (1971)].
- ³⁷I. I. Komissarova and G. V. Ostrovskaya, *Proc. of the First All-Union Conference on Holography, Problems of Holography, Moscow, 1973*, V. 3, p. 50.
- ³⁸Kh. P. Alum, Yu. V. Koval'chuk, and G. V. Ostrovskaya, *Pis'ma Zh. Tekh. Fiz.* **7**, 1359 (1981) [*Sov. Tech. Phys. Lett.* **7**, 583 (1981)]; Author's certificate 864942 (1981); *Byuleten' isobretatelya* (Inventor's Bulletin), No. 35, 274 (1983).
- ³⁹F. A. Hopf, A. Tomito, and G. Al-Jumaily, *Opt. Lett.* **5**, 38 (1980).
- ⁴⁰Kh. P. Alum, Yu. V. Koval'chuk, and G. V. Ostrovskaya, *Zh. Tekh. Fiz.* **54**, 896 (1984) [*Sov. Phys. Tech. Phys.* **29**, 534 (1984)].
- ⁴¹D. Nobis and D. M. Vest, *Appl. Opt.* **17**, 2198 (1978).
- ⁴²I. I. Komissarova, G. V. Ostrovskaya, V. N. Filippov, and E. N. Shedova, same as Ref. 23.
- ⁴³P. R. Forman, S. Humphries, and K. W. Peterson, *Appl. Phys. Lett.* **22**, 537 (1973).
- ⁴⁴A. Darr, G. Decker, and H. Rohr, *Z. Phys.* **248**, 121 (1971).
- ⁴⁵W. Braun, *Phys. Lett.* **A47**, 144 (1974); *Z. Phys.* **20**, 195 (1975).
- ⁴⁶G. Decker, H. Harold, and H. Rohr, *Appl. Phys. Lett.* **20**, 490 (1972).
- ⁴⁷P. R. Forman, F. C. Jahoda, and R. W. Peterson, *Appl. Opt.* **20**, 477 (1972).
- ⁴⁸B. P. Zakharchenya, F. A. Chudnovskii, and Z. I. Steingolz, *Pis'ma Zh. Tekh. Fiz.* **9**, 76 (1983) [*Sov. Tech. Phys. Lett.* **9**, 32 (1983)].
- ⁴⁹D. Naor, A. Flusberg, and I. Itzkan, *Appl. Opt.* **20**, 2574 (1981).
- ⁵⁰I. Ursu, D. Apostol, I. Apostol *et al.*, *Zh. Tekh. Fiz.* **52**, 1432 (1982) [*Sov. Phys. Tech. Phys.* **27**, 873 (1982)].
- ⁵¹*Dye Lasers*, Ed. F. P. Schäfer, Springer-Verlag, Berlin, 1977 (Topics in Applied Physics, V. 1) [Russ. Transl., Mir, M., 1976].
- ⁵²B. G. Belostotskii, Yu. V. Lyubavskii, and V. M. Ovchinnikov, *Osnovy lazernoĭ tekhniki* (Fundamentals of laser technique), *Sov. Radio*, M., 1972.
- ⁵³W. W. Duley, *CO₂-Lasers' Effects and Applications*, Academic Press, London, N. Y., 1976.
- ⁵⁴R. Kristal, *Appl. Opt.* **14**, 628 (1975).
- ⁵⁵A. N. Zaidel', G. V. Ostrovskaya, Yu. I. Ostrovskii, and T. Ya. Chelidze, *Zh. Tekh. Fiz.* **36**, 2208 (1966) [*Sov. Phys. Tech. Phys.* **11**, 1650 (1967)].
- ⁵⁶L. H. Tanner, *J. Sci. Instrum.* **41**, 81 (1966).
- ⁵⁷R. S. Thomas, C. R. Harder, W. E. Quinn, and R. E. Siemon, *Phys. Fluids* **15**, 1658 (1972).
- ⁵⁸Yu. V. Afanas'ev, N. B. Basov, O. N. Krokhin *et al.*, *Zh. Tekh. Fiz.* **39**, 894 (1969) [*Sov. Phys. Tech. Phys.* **14**, 669 (1969)].
- ⁵⁹Yu. I. Ostrovskii, Author's certificate 179188 (1963), *Inventor's Bulletin*, No. 14, 1970; *Opt. Spektrosk.* **21**, 620 (1966) [*Opt. Spectrosc.* (USSR) **21**, 342 (1970)].
- ⁶⁰T. Tschudi, C. Yamanaka, T. Sasaki *et al.*, *J. Phys.* **D11**, 177 (1978).
- ⁶¹O. N. Krokhin, *Laser Handbook*, North-Holland, Amsterdam, 1970, Secs. 5, 7.
- ⁶²N. G. Basov, V. A. Gribkov, O. N. Krokhin, and G. V. Sklizkov, *Zh. Tekh. Fiz.* **54**, 1973 (1968) [*sic*].
- ⁶³G. V. Sklizkov, Application of lasers for very high speed investigation of fast processes (Primenenie lazerov dlya svekhskorostnogo issledovaniya bystroprotekeyushchikh protsessov): Preprint of FIAN USSR, Moscow, #29, 1970.
- ⁶⁴R. D. Herriot and H. J. Schultze, *Appl. Opt.* **4**, 583 (1965).
- ⁶⁵A. G. Smirnov, V. G. Smirnov, and D. I. Stasel'ko, NIIIEFA T-0171 Preprint, Leningrad, 1972.
- ⁶⁶A. T. Ellis and M. E. Fourny, *Proc. IEEE* **51**, 942 (1963).
- ⁶⁷A. N. Zaidel and Yu. I. Ostrovsky, see Ref. 10.
- ⁶⁸J. W. Gates, *Nature* **220**, 473 (1968).
- ⁶⁹G. V. Ostrovskaya and A. N. Zaidel', *Usp. Fiz. Nauk* **111**, 579 (1973) [*Sov. Phys. Usp.* **16**, 834 (1974)].
- ⁷⁰I. I. Komissarova, T. V. Ostrovskaya, and L. L. Shapiro, *Zh. Tekh. Fiz.* **38**, 1369 (1968) [*Sov. Phys. Tech. Phys.* **13**, 1118 (1969)].
- ⁷¹A. N. Zaidel', I. I. Komissarova, G. V. Ostrovskaya, and L. L. Shapiro, Holographic studies of laser sparks with the aid of the fundamental and second harmonic frequencies of a ruby laser (in Russian), FTIAN SSSR Preprint #182, Leningrad, 1969.
- ⁷²I. I. Komissarova, G. V. Ostrovskaya, and L. L. Shapiro, Holographic studies of laser sparks in air, Preprint of Physico-Technical Institute of the Academy of Sciences of the USSR, #226, Leningrad, 1969.
- ⁷³A. B. Ignatov, I. I. Komissarova, G. V. Ostrovskaya, and L. L. Shapiro, *Zh. Tekh. Fiz.* **41**, 701 (1971) [*Sov. Phys. Tech. Phys.* **16**, 550 (1971)].
- ⁷⁴I. I. Komissarova and G. V. Ostrovskaya, *Zh. Tekh. Fiz.* **48**, 2062 (1978) [*Sov. Phys. Tech. Phys.* **23**, 1176 (1978)].
- ⁷⁵Kh. P. Alum, Yu. V. Koval'chuk, and G. V. Ostrovskaya, *Zh. Tekh. Fiz.* **51**, 1618 (1981) [*Sov. Phys. Tech. Phys.* **26**, 928 (1981)].
- ⁷⁶G. V. Ostrovskaya and N. A. Pobedonostseva, *Zh. Tekh. Fiz.* **45**, 1462 (1975) [*Sov. Phys. Tech. Phys.* **20**, 923 (1975)].
- ⁷⁷Yu. Koval'chuk, I. I. Komissarova, and G. V. Ostrovskaya, *Zh. Tekh. Fiz.* **49**, 2637 (1979) [*Sov. Phys. Tech. Phys.* **24**, 1489 (1979)].
- ⁷⁸See Ref. 26.
- ⁷⁹E. M. Barchudarov, V. K. Berezovskii, and T. Ya. Tchelidze, *J. Phys. (Paris) Colloq.* **40**, C7-869 (1979).
- ⁸⁰J. C. Buges, A. Plet, and A. Termeaud, *C. R. Acad. Sci.* **267**, 1271 (1968).
- ⁸¹J. L. Bobin, J. C. Buges, P. Rouzard *et al.*, *Proc. of 9th Intern. Conference on Phenomena of Ionized Gases*, Bucharest, 1969.
- ⁸²W. K. Pendelton Guenther, C. Smith *et al.*, *J. Opt. Soc. Am.* **61**, 688 (1971); *Opt. Laser Technol.* **5**, 20 (1973).
- ⁸³A. Giulietti, D. Giulietti, M. Luchesi, and I. Vasselli, *Opt. Commun.* **47**, 131 (1983).
- ⁸⁴R. Sied, *Phys. Lett.* **A30**, 103 (1969); *Z. Naturforsch.* **25**, 488 (1970).
- ⁸⁵I. I. Ashmarin, Yu. A. Bykovskii, N. N. Degtyarenko *et al.*, *Zh. Tekh. Fiz.* **41**, 2369 (1971) [*Sov. Phys. Tech. Phys.* **16**, 1881 (1972)].
- ⁸⁶R. Belland, C. DeMichelis, and M. Mattioli, *Opt. Commun.* **3**, 7 (1971).
- ⁸⁷See Ref. 30.
- ⁸⁸G. V. Dreiden, G. V. Ostrovskaya, N. A. Pobedonostseva, and V. N. Filippov, *Pis'ma Zh. Eksp. Teor. Fiz.* **1**, 106 (1975) [*JETP Lett.* **1**, 48 (1975)].
- ⁸⁹D. R. Koopman, H. J. Sibeneck, G. Jellison, and W. G. Niessen, *Rev. Sci. Instrum.* **49**, 254 (1978).
- ⁹⁰S. Yu. Luk'yanov, D. A. Shcheglov, V. E. Golant, M. P. Petrov, V. S. Zaveryaev, and N. G. Koval'skii, *Diagnostika termoyadernoi plasmy* (Diagnostics of Thermonuclear Plasma), *Energoatomizdat*, M., 1985.
- ⁹¹J. N. Olsen and C. W. Mendel, *J. Appl. Phys.* **46**, 4407 (1975).
- ⁹²D. T. Attwood and L. W. Coleman, *Appl. Phys. Lett.* **24**, 408a (1974); **26**, 616 (1975).
- ⁹³D. W. Sweeney, D. T. Attwood, and L. W. Coleman, *Appl. Opt.* **15**, 1126 (1976).
- ⁹⁴D. T. Attwood, *IEEE J. Quantum Electron.* **QE-14**, 909 (1978).
- ⁹⁵D. T. Attwood, E. L. Pierce, D. W. Sweeney *et al.*, *Picosecond Phenomena*/Eds. C. V. Shank *et al.*, Springer-Verlag, Berlin; Heidelberg; New York, 1978, p. 293.
- ⁹⁶E. L. Pierce, *Appl. Opt.* **19**, 952 (1980).
- ⁹⁷M. D. J. Burgess, G. B. Gillman, and B. Luther-Davis, *J. Appl. Phys.* **54**, 1787 (1983).
- ⁹⁸C. J. Tallents, M. D. J. Burgess, and B. Luther-Davis, *Opt. Commun.* **44**, 384 (1983).
- ⁹⁹G. V. Dreiden, A. N. Zaidel', V. S. Markov *et al.*, *Pis'ma Zh. Tekh. Fiz.* **1**, 141 (1975) [*Sov. Tech. Phys. Lett.* **1**, 68 (1975)].
- ¹⁰⁰G. V. Dreiden, N. P. Kirii, V. S. Markov, A. Mirasabekov, G. V. Ostrovskaya, A. G. Frank, A. Z. Khodzhaev, and E. N. Shedova, *Fiz. Plasmy* **3**, 45 (1977) [*Sov. J. Plasma Phys.* **3**, 26 (1977)].
- ¹⁰¹G. V. Dreiden, V. S. Markov, and G. V. Ostrovskaya, *ibid.* **4**, 14 (1978) [*Sov. J. Plasma Phys.* **4**, 6 (1978)].
- ¹⁰²G. V. Dreiden, I. I. Komissarova, V. S. Markov *et al.*, *Zh. Tekh. Fiz.* **51**, 1850 (1981) [*Sov. Phys. Tech. Phys.* **26**, 1072 (1981)]; The study of spatial and temporal variations of electron concentrations during fast changes of the magnetic field structure of the current layer: FIAN Preprint (USSR), No. 35, Moscow, 1980.

- ¹⁰³A. G. Smirnov, *Opticheskaya golografiya i ee primeneniya* (Optical holography and its applications), LDNTP, Leningrad, 1974, p. 45.
- ¹⁰⁴L. G. Dubovoi, A. G. Smirnov, V. G. Smirnov *et al.*, *ibid.*, p. 47.
- ¹⁰⁵V. V. Bryskin and A. G. Smirnov, *ibid.*, p. 50.
- ¹⁰⁶F. C. Jahoda, Ref. 10, p. 109.
- ¹⁰⁷A. Bernard, J. C. Buges, A. Jolics *et al.*, 4th European Conference on Controlled Fusion and Plasma Physics, Rome, 1970, p. 52.
- ¹⁰⁸F. Gribble, W. E. Quinn, and R. B. Siemon, *Phys. Fluids* **14**, 2042 (1971).
- ¹⁰⁹K. S. Thomas, C. R. Harder, W. E. Quinn *et al.*, *ibid.* **15**, 1658 (1972).
- ¹¹⁰K. H. Finken and U. Ackerman, *J. Phys.* **D16**, 773 (1983).
- ¹¹¹V. A. Nikashin, G. Ya. Rukman, V. V. Sakharov *et al.*, *Teplotiz. Vys. Temp.* **7**, 1198 (1969).
- ¹¹²V. M. Ginzburg, B. M. Stepanov, and Yu. I. Filenko, *Radiotekh. Elektron.* **17**, 2219 (1972) [*Radio Eng. Electron. (USSR)* **17**, 1781 (1972)].
- ¹¹³V. A. Burtsev, A. A. Kondakov, and V. P. Ponogin, *Zh. Tekh. Fiz.* **48**, 712 (1978) [*Sov. Phys. Tech. Phys.* **23**, 419 (1978)].
- ¹¹⁴V. A. Burtsev, L. A. Zelenov, A. A. Kondakov *et al.*, *J. Phys. (Paris) Colloq.* **40**, C7-387 (1979).
- ¹¹⁵V. A. Burtsev, L. A. Zelenov, A. A. Kondakov *et al.*, *Proc. of the 3rd All-Union Conference on Holography*, Ul'yanovsk, 1978, p. 143.
- ¹¹⁶L. V. Sutter, P. K. Baily, and G. Wakalopoulos *et al.*, *Appl. Opt.* **18**, 2835 (1979).
- ¹¹⁷V. A. Burtsev, A. A. Kondakov, R. F. Kurunov *et al.*, *Experimental investigation of instabilities in non-self-sustained discharges*, NIIÉFA, Preprint No. P-K-0481, Leningrad, 1980.
- ¹¹⁸L. A. Zelenov, N. A. Kamarudin, R. F. Kurunov *et al.*, *Studies of the development of self-sustained discharges in molecular gases by methods of holographic interferometry*, Preprint No. P-K-0598, NIIÉFA, Leningrad, 1982.
- ¹¹⁹L. A. Zelenov, R. F. Kurunov, V. K. Ratkevich *et al.*, *Experimental investigations of gasodynamic processes in 3-dimensional non-self-sustained discharge by the method of holographic interferometry*, Preprint No. P-K-0481, NIIÉFA, Leningrad, 1980.
- ¹²⁰A. P. Burmakov and G. V. Ostrovskaya, *Zh. Tekh. Fiz.* **40**, 660 (1970) [*Sov. Phys. Tech. Phys.* **15**, 514 (1970)].
- ¹²¹A. P. Burmakov, A. A. Labuda, V. M. Lutkovskii, *Inzh.-Fiz. Zh.* **29**, 499 (1975).
- ¹²²F. C. Jahoda, *Appl. Phys. Lett.* **17**, 341 (1969).
- ¹²³A. P. Burmakov and A. G. Shashkov, *Properties of low-temperature plasma and methods for its diagnostics*, Nauka, Novosibirsk, 1977, p. 216.
- ¹²⁴Yu. P. Raizer, *Lazernaga iskra i rasprostranenie razryadov*, Nauka, M., 1974 [Engl. Transl., *Laser-induced discharge phenomena*, Consultants Bureau, N. Y., 1977].
- ¹²⁵R. J. Radley, Jr., *Phys. Fluids* **18**, 175 (1975).
- ¹²⁶M. V. Gerasimenko and G. I. Korlov, *Plasma physics*, Moscow, 9, p. 1269, Energoatomizdat (1983).
- ¹²⁷R. A. Jeffries, *Phys. Fluids* **13**, 110 (1970).
- ¹²⁸E. A. Antonov, L. N. Gnat'yuk, B. I. Stepanov *et al.*, *Teplotiz. Vys. Temp.* **10**, 1210 (1972); *Prib. Tekh. Eksp. No. 3*, 212 (1972).
- ¹²⁹U. Kogal'shatts, in Ref. 123, p. 193.
- ¹³⁰B. Inaichen, U. Kogelschatz, and R. Daudliker, *Appl. Opt.* **12**, 2554 (1973).
- ¹³¹J. Blass, XVI Intern. Conference on Ionized Gases, Dusseldorf, 1983, p. 422.
- ¹³²Y. I. Filenko, B. M. Stepanov, and D. S. Ushakov, *J. Phys. (Paris) Colloq.* **40**, C7-873 (1979).
- ¹³³L. Horton and R. M. Gilgenbach, *Appl. Phys. Lett.* **43**, 1010 (1983).
- ¹³⁴V. A. Burtsev, L. A. Zelenov, N. A. Kamarudin *et al.*, Ref. 131, p. 144.
- ¹³⁵V. A. Burtsev, A. A. Kondakov, R. F. Kurunov *et al.*, XV Intern. Conference on Ionized Gases, Minsk, 1981.
- ¹³⁶L. A. Zelenov, R. F. Kurunov, V. K. Radkevich, and V. G. Smirnov, Ref. 131, p. 144.
- ¹³⁷A. M. Mirzabekov, N. K. Mitrofanov, Yu. I. Ostrovskii, and E. N. Shedova, *Opt. Spektrosk.* **51**, 2038 (1981) [*sic*].
- ¹³⁸A. G. Zhiglinskii, G. G. Kund, and A. O. Morozov, *ibid.* **46**, 1196 (1979) [**46**, 675 (1979)].
- ¹³⁹A. G. Zhiglinskii, A. O. Morozov, A. N. Samokhin *et al.*, *Fizicheskiye osnovy golografii* (Physical basis of holography), Institute of Nuclear Physics of the Academy of Sciences of the USSR, Leningrad, 1981, p. 74.
- ¹⁴⁰K. S. Mustafin, V. I. Protasevich, and V. N. Rzhetskaya, *Opt. Spektrosk.* **30**, 106 (1971) [*sic*].
- ¹⁴¹N. P. Datskevich, N. V. Karlov, N. N. Kononov *et al.*, *Kratkie soobshcheniya po fizike* (Brief notes on physics) (FIAN) SSSR No. 3, 52 (1984).
- ¹⁴²N. P. Datskevich, N. V. Karlov, N. N. Kononov *et al.*, *Fiz. Plasmy* **10**, 762 (1984) [*Sov. J. Plasma Phys.* **10**, 442 (1984)].
- ¹⁴³N. P. Datskevich, N. V. Karlov, N. N. Kononov *et al.*, *Kvantovaya Elektron. (Moscow)* **11**, 853 (1984) [*Sov. J. Quantum Electron.* **14**, 579 (1984)].
- ¹⁴⁴N. V. Datskevich, N. V. Karlov, N. N. Kononov *et al.*, *ibid.* **12**, 2029 (1985) [*Sov. J. Quantum Electron.* **15**, 1338 (1985)].
- ¹⁴⁵G. R. Toker, *Pulsed two-exposure holographic interferometry of CO₂-laser plasma* (in Russian), IOFAN SSSR Preprint No. 257, Moscow, 1985.
- ¹⁴⁶E. M. Barkhudarov, G. V. Gelashvili, G. G. Gumberidze *et al.*, *Fiz. Plasmy* **10**, 757 (1984) [*Sov. J. Plasma Phys.* **10**, 439 (1984)].

Translated by A. Petelin